

$[\text{CII}]_{158\mu\text{m}}$ and $[\text{NII}]_{205\mu\text{m}}$ emission in IC 342

M. Röllig, R. Simon, R. Güsten, J. Stutzki, F. Israel, and K. Jacobs

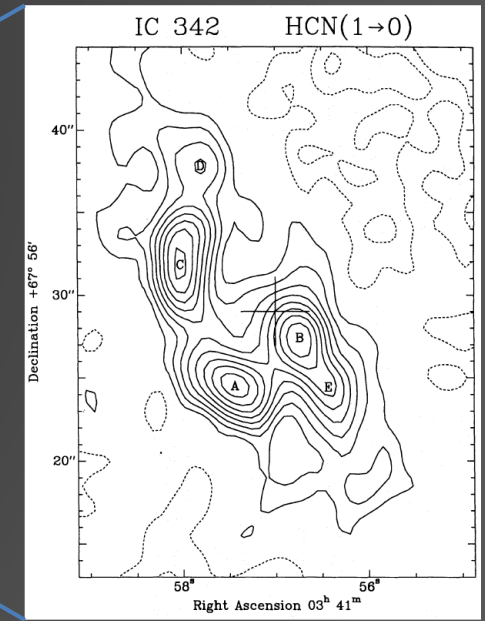
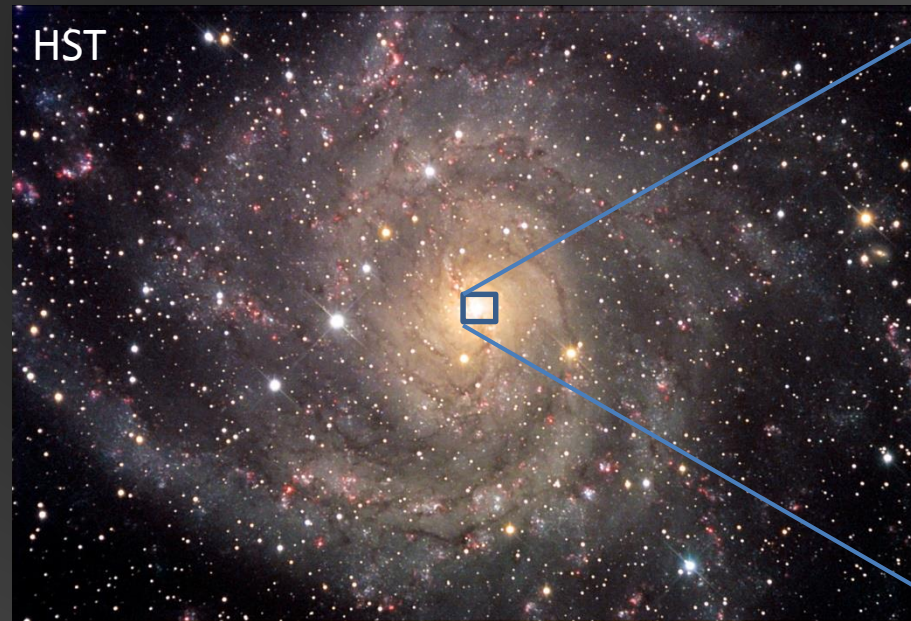
Universität zu Köln, Germany

Introduction

NASA/JPL-Caltech/UCLA -

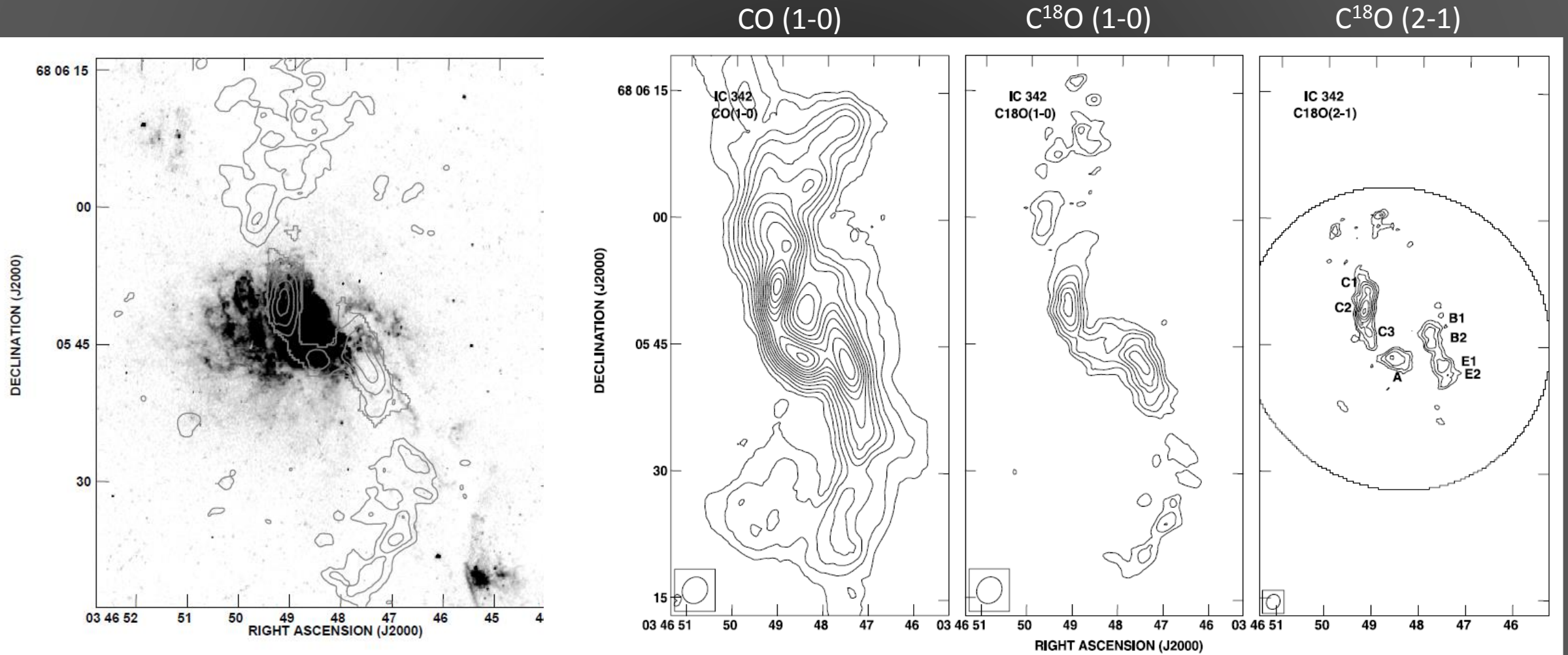


- Barred spiral obscured by the plane of the MW
- $D=3.3$ Mpc
- Starburst activity in the center
- Sometimes considered a „close relative“ to the MW



Downes et al. 1992

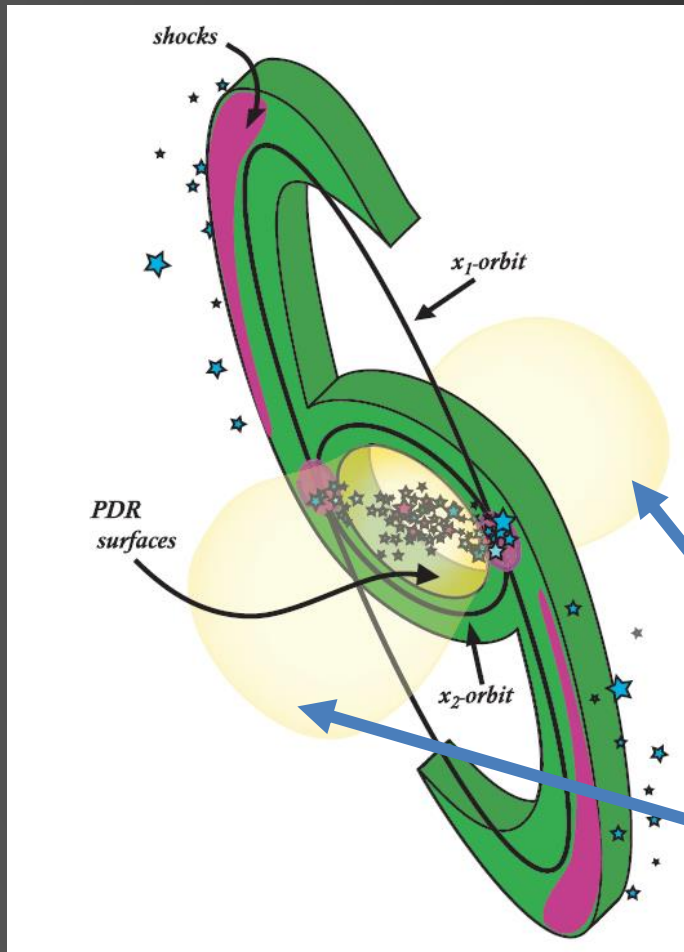
The Nucleus of IC 342



$N(\text{H}_2)$ on HST H α

Meier & Turner 2001

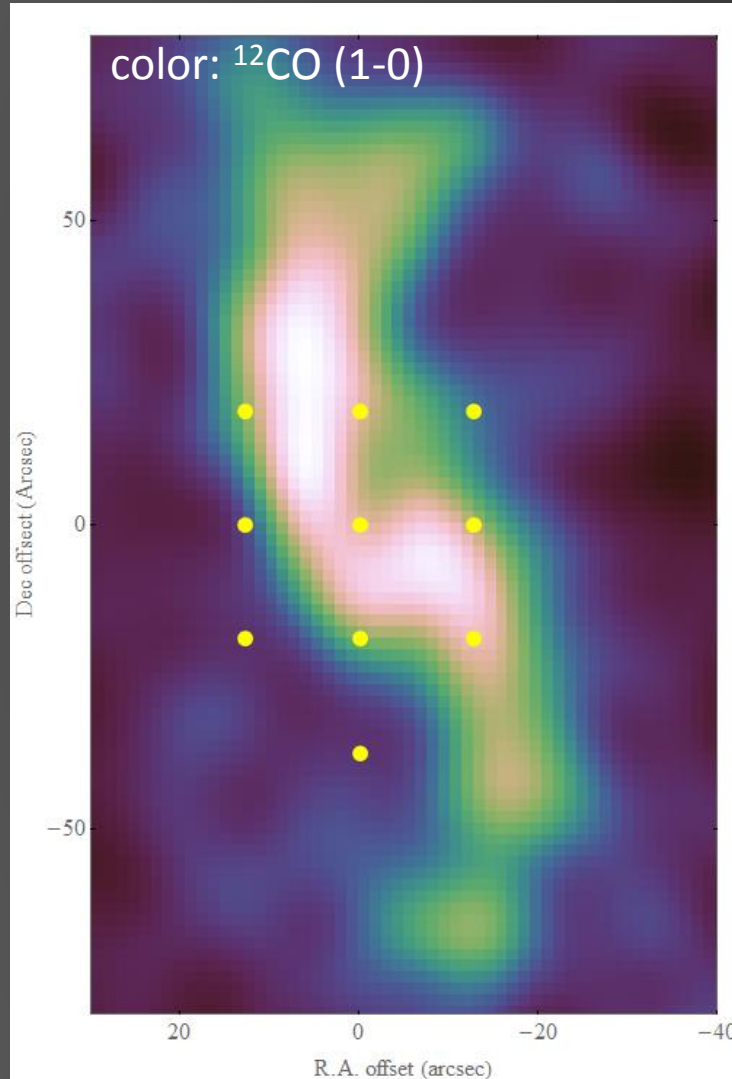
IC 342 – Geometry of the inner 300pc



Meier & Turner 2005

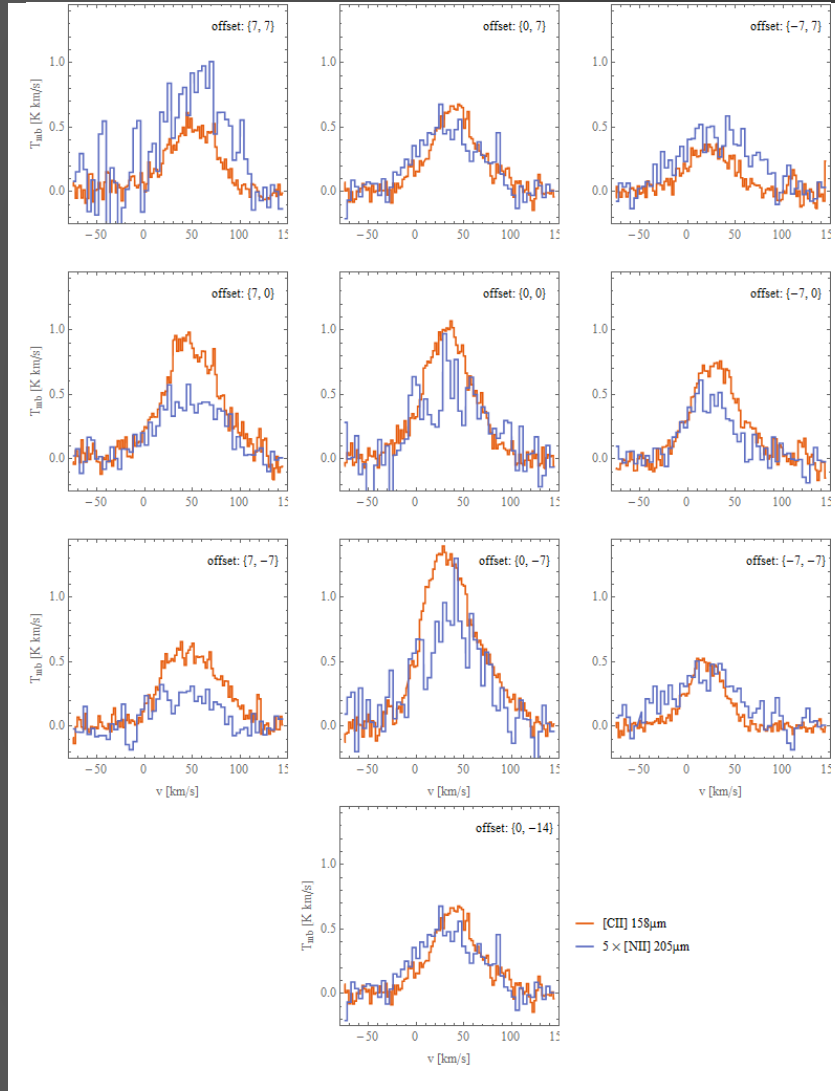
- Bar-potential leads to mini-spiral configuration in the nucleus
- The spiral arms end at an inner molecular ring
- The center of the ring is dominated by an evolved (60 Myr) massive star cluster
- The inner rim of the ring is illuminated by FUV → PDR emission
- Expanding bubbles of HII gas

SOFIA/GREAT observations 2013/14



- 10 positions (spacing 7'') in dual-beam switch mode observed during 3 flights
- L1/L2 GREAT configuration
 - L1: [NII] $^3P_1 - ^3P_0$ 205 μm
 - L2: [CII] $^3P_{3/2} - ^3P_{1/2}$ 158 μm
- $t_{\text{ON}} = 2.5\text{min} - 7.5\text{min}$
- $T_{\text{sys}} = 2000\text{--}5500\text{ K}$
- 8192 channel FFTS with 1.5 GHz bandwidth and 212 kHz spectral resolution

SOFIA/GREAT observations 2013/14



- 10 positions (spacing 7'') in dual-beam switch mode observed during 3 flights
- L1/L2 GREAT configuration

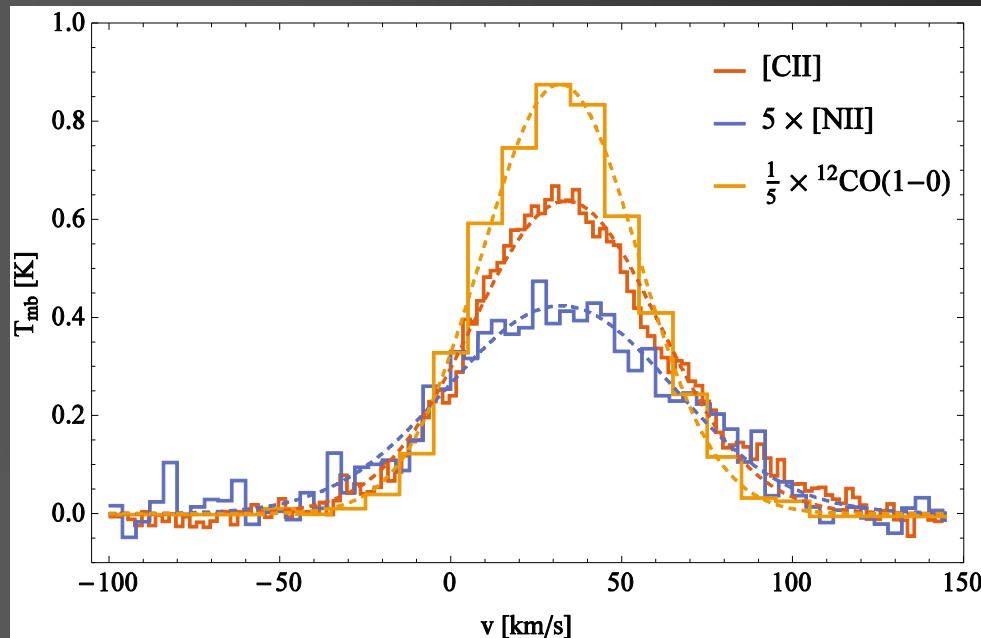
L1: [NII] 3P_1 - 3P_0	205μm
L2: [CII] $^3P_{3/2}$ - $^3P_{1/2}$	158μm
- $t_{\text{ON}}=2.5\text{min} - 7.5\text{min}$
- $T_{\text{sys}}=2000\text{-}5500\text{ K}$
- 8192 channel FFTS with 1.5 GHz bandwidth and 212 kHz spectral resolution
- $\text{RMS}_{[\text{NII}]} < 100\text{mK}$
 $\text{RMS}_{[\text{CII}]} < 60\text{mK}$

red: [CII], blue: [NII] $\times 5$

[CII] and [NII] emission in IC342 - The 6th Zermatt ISM Symposium - 7. Sep. 2015

SOFIA/GREAT observations 2013/14

average spectrum over central 3x3

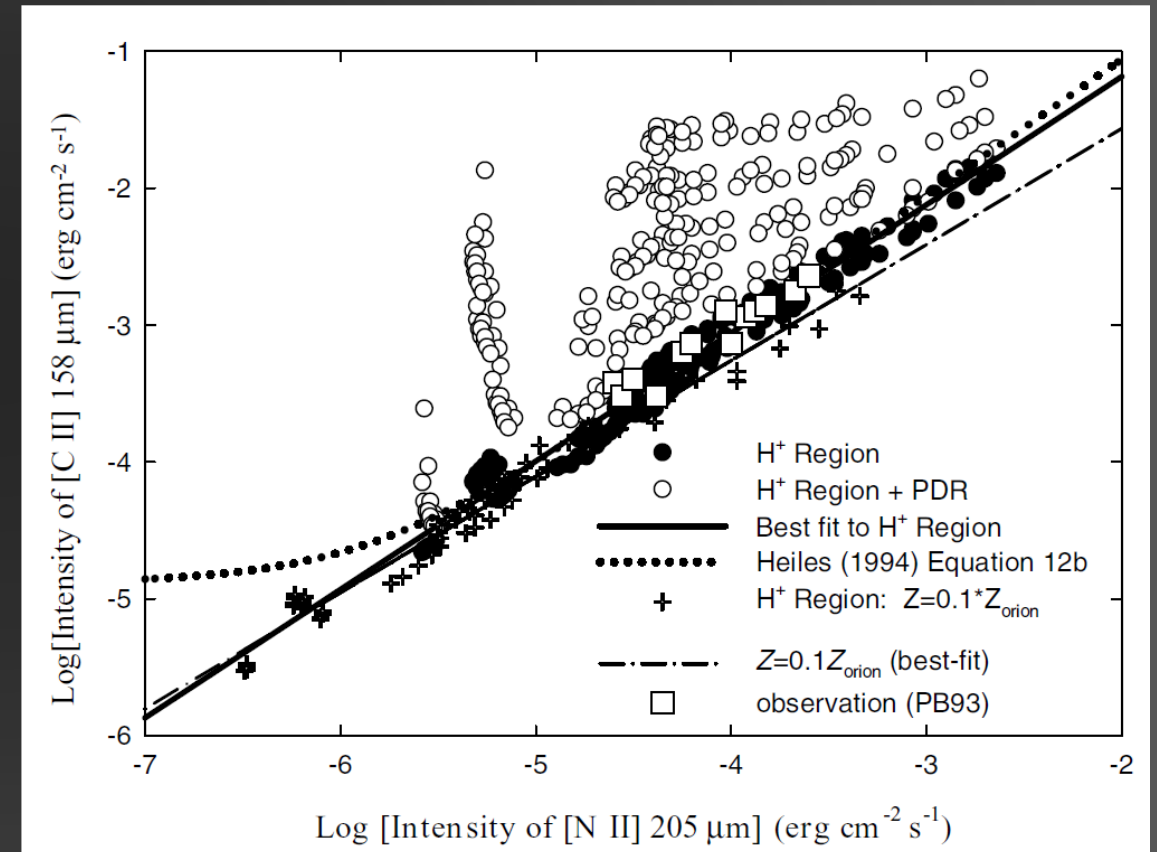


- 10 positions (spacing 7'') in dual-beam switch mode observed during 3 flights
- L1/L2 GREAT configuration
 - L1: [NII] $^3P_1 - ^3P_0$ 205 μm
 - L2: [CII] $^3P_{3/2} - ^3P_{1/2}$ 158 μm
- $t_{\text{ON}} = 2.5\text{min} - 7.5\text{min}$
- $T_{\text{sys}} = 2000\text{-}5500\text{ K}$
- 8192 channel FFTS with 1.5 GHz bandwidth and 212 kHz spectral resolution
- $\text{RMS}_{[\text{NII}]} < 100\text{mK}$
 $\text{RMS}_{[\text{CII}]} < 60\text{mK}$

[CII] – [NII] correlation

- $IP(N) = 14.53 \text{ eV}$
- FUV energy in PDRs $6\text{eV} < h\nu < 13.6 \text{ eV}$
- **[NII] is always emitted from HII regions**
- $IP(C) = 11.3 \text{ eV}$
- Carbon in HII regions is in the form C^+ and C^{2+}
- Carbon in PDRs is layered $C^+/C/CO$
- **[CII] is emitted from PDRs and HII regions**

What fraction of [CII] is from which phase?

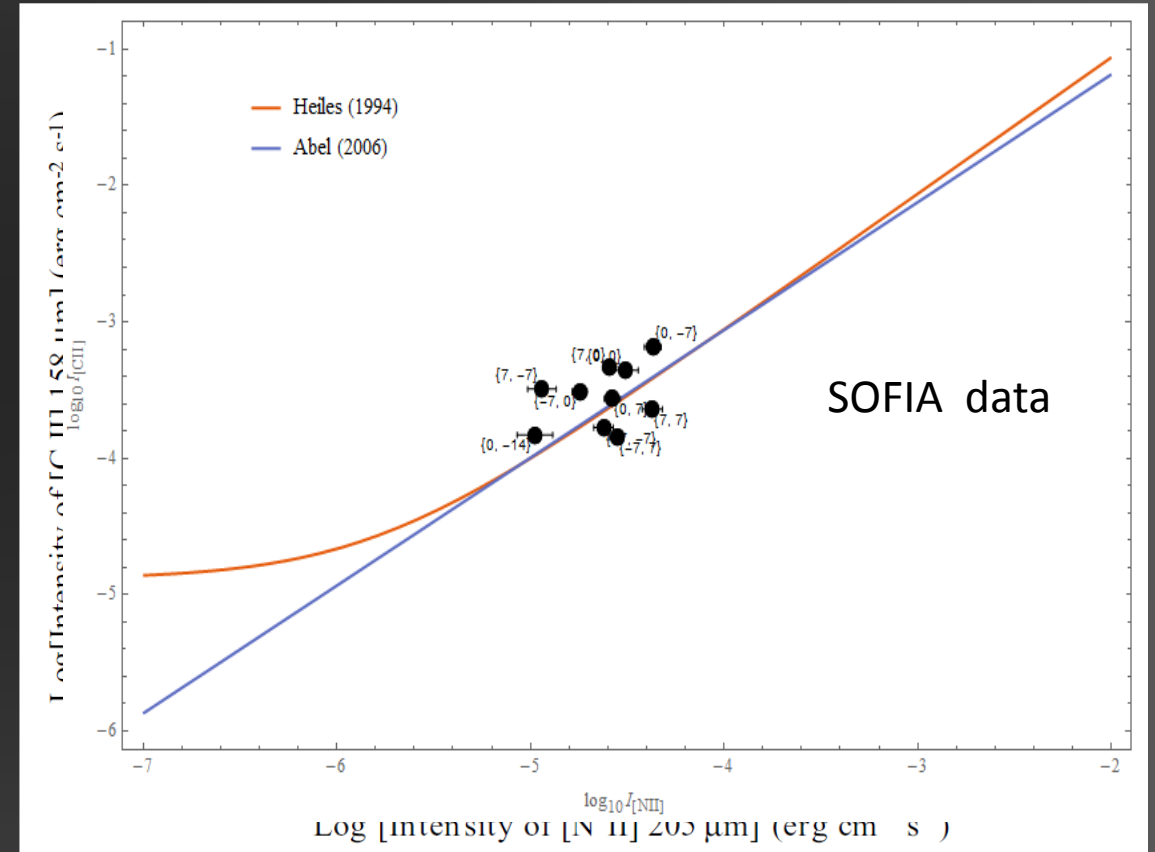


Abel 2006

[CII] – [NII] correlation

- $IP(N) = 14.53 \text{ eV}$
- FUV energy in PDRs $6\text{eV} < h\nu < 13.6 \text{ eV}$
- **[NII] is always emitted from HII regions**
- $IP(C) = 11.3 \text{ eV}$
- Carbon in HII regions is in the form C^+ and C^{2+}
- Carbon in PDRs is layered $C^+/C/CO$
- **[CII] is emitted from PDRs and HII regions**

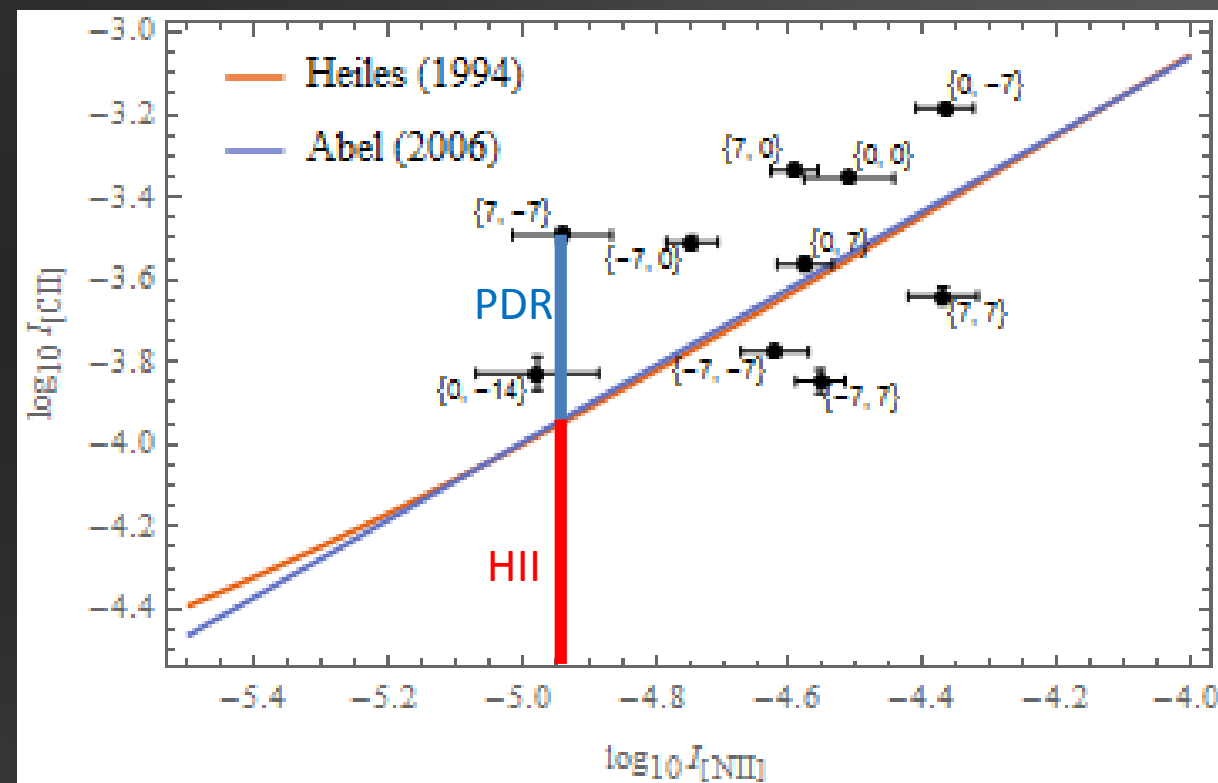
What fraction of [CII] is from which phase?



Abel 2006

[CII] – [NII] correlation in IC 342

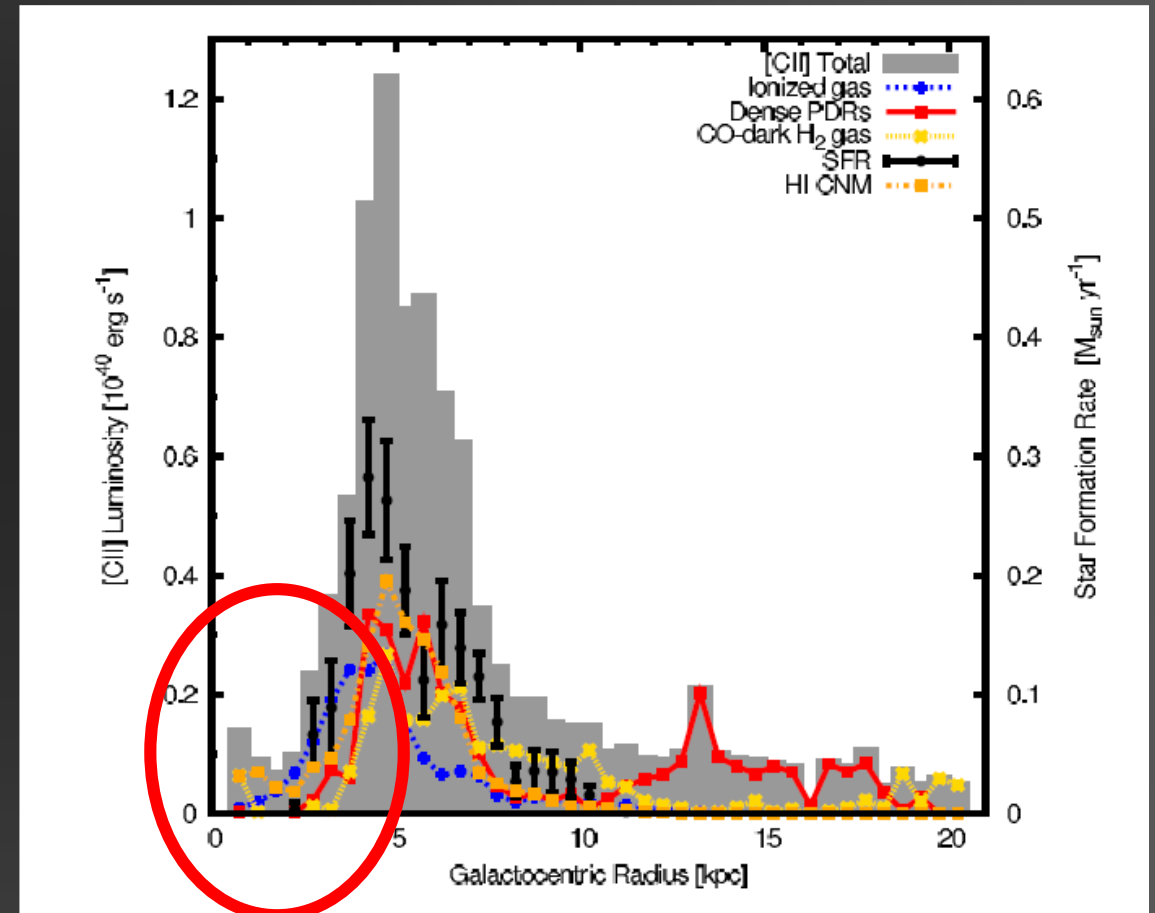
- 3 positions: only $[\text{CII}]_{\text{HII}}$
- 7 positions: $[\text{CII}]_{\text{HII}} \sim 35\text{-}90\% [\text{CII}]_{\text{tot}}$
- Quite high values:
MW average $[\text{CII}]_{\text{HII}} \sim 20\%$, $[\text{CII}]_{\text{PDR}} \sim 30\%$



Röllig et al. 2015

[CII] – [NII] correlation in IC 342

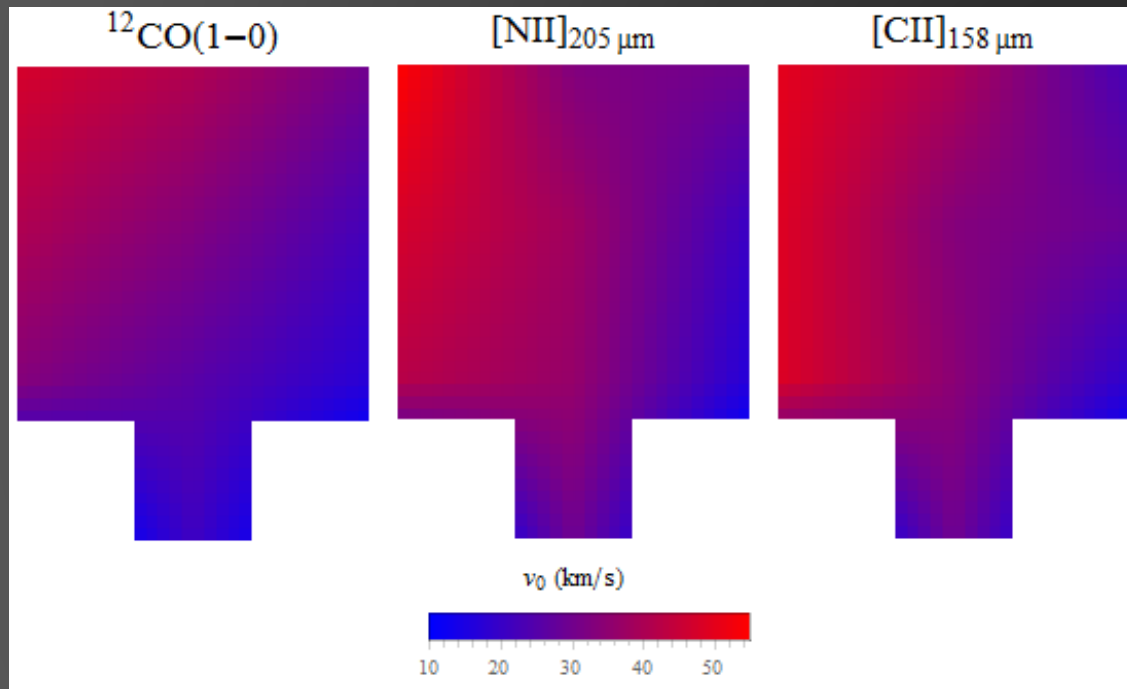
- 3 positions: only $[\text{CII}]_{\text{HII}}$
- 7 positions: $[\text{CII}]_{\text{HII}} \sim 35\text{-}90\% [\text{CII}]_{\text{tot}}$
- Quite high values:
MW average $[\text{CII}]_{\text{HII}} \sim 20\%$, $[\text{CII}]_{\text{PDR}} \sim 30\%$
- But: inner kpc of the MW also shows $[\text{CII}]_{\text{HII}} > [\text{CII}]_{\text{PDR}}$
- Both, IC 342 and MW show a strong contribution of $[\text{CII}]_{\text{HII}}$ to $[\text{CII}]_{\text{tot}}$ in their center.



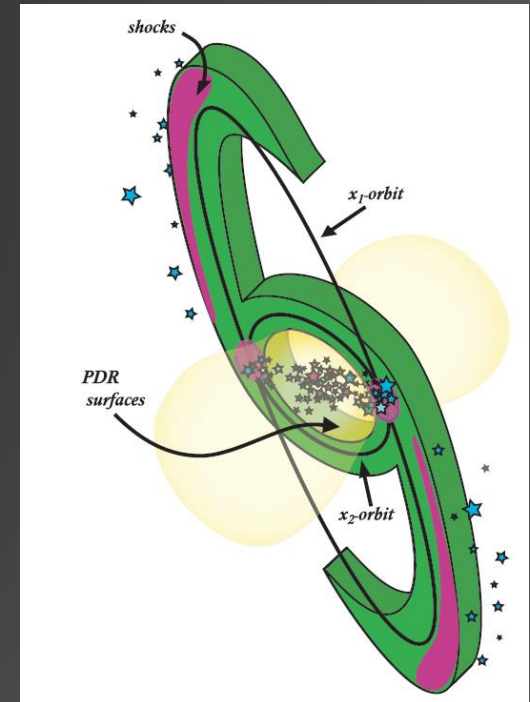
Pineda et al. 2014

Kinematics: [CII], [NII] and $^{12}\text{CO}(1-0)$

line center velocities

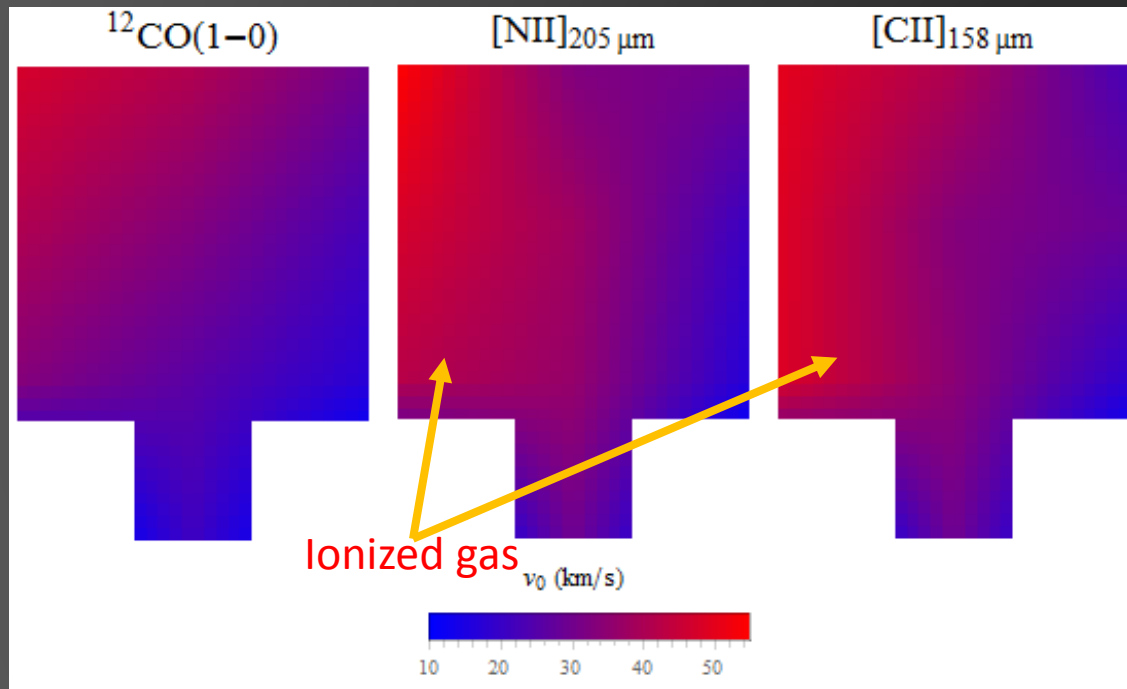


- Gaussian line center velocities show spatial differences between CO, C^+ and N^+
- CO shows a clear velocity gradient from N-E to S-W

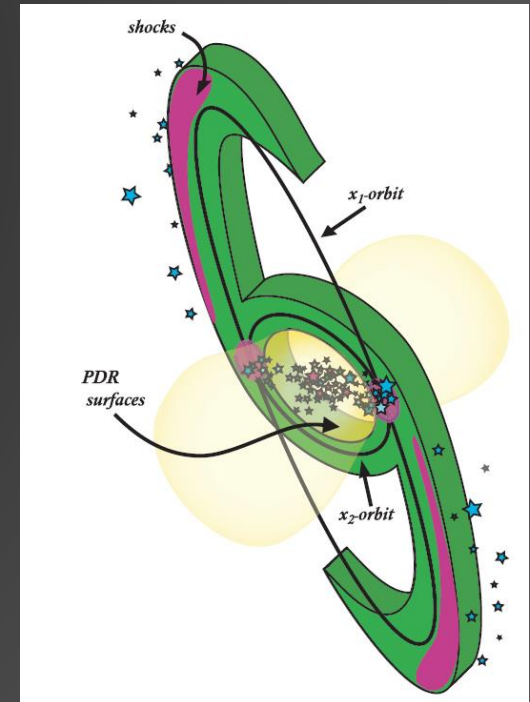


Kinematics: [CII], [NII] and $^{12}\text{CO}(1-0)$

line center velocities

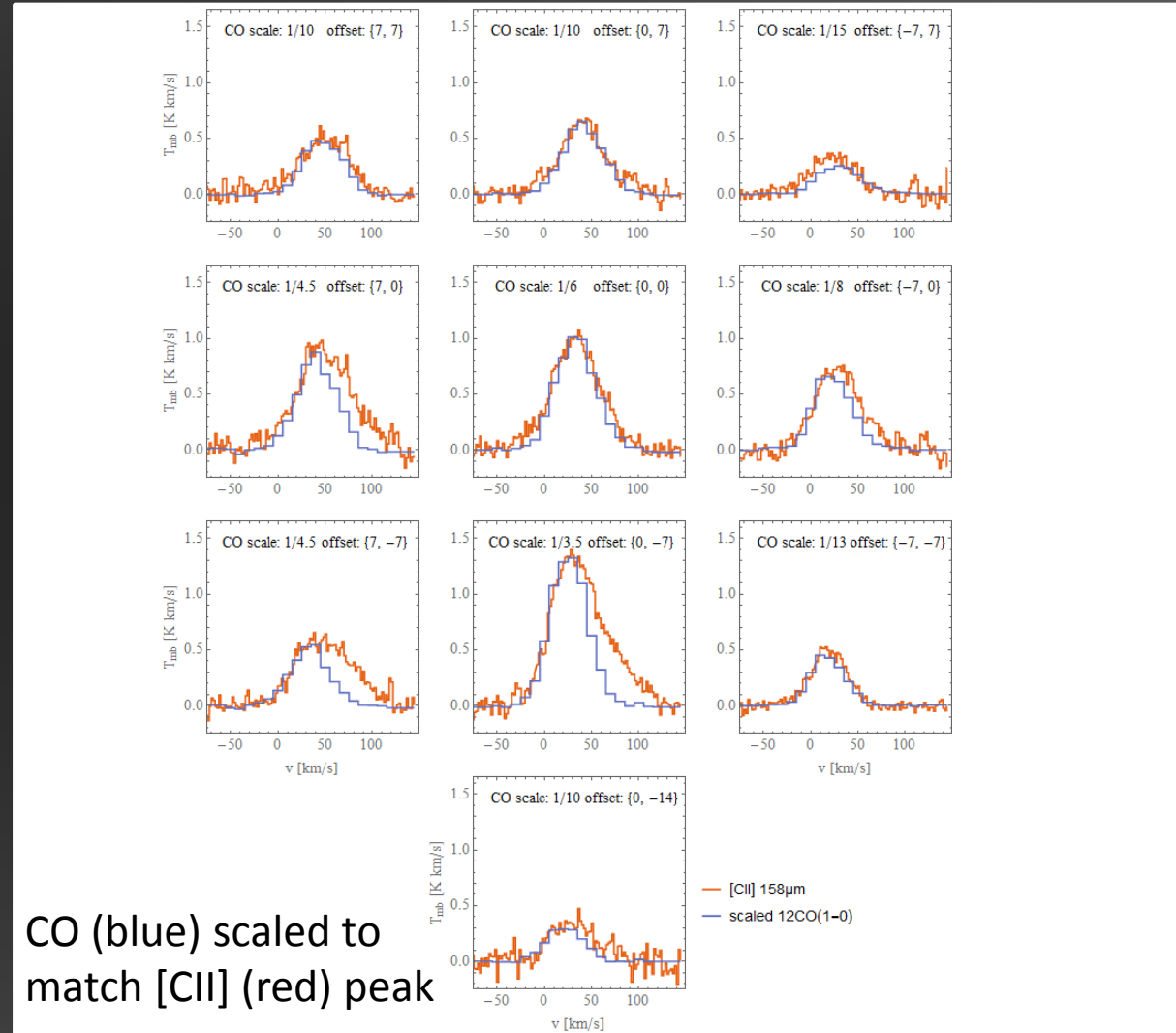
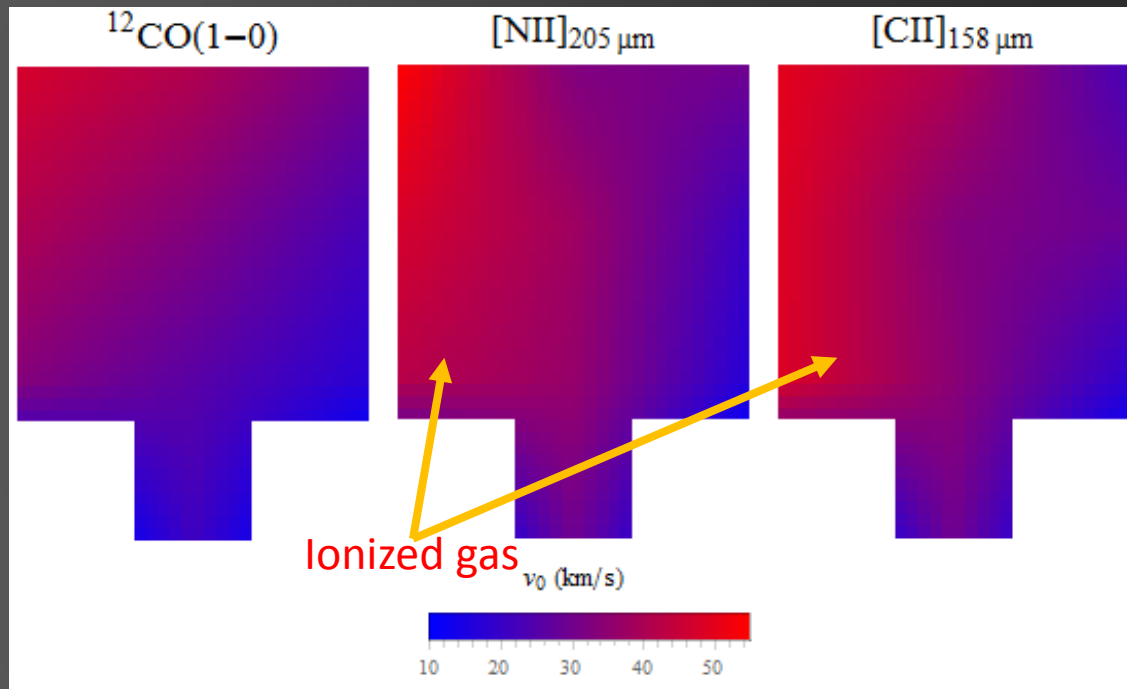


- Gaussian line center velocities show spatial differences between CO, C⁺ and N⁺
- CO shows a clear velocity gradient from N-E to S-W



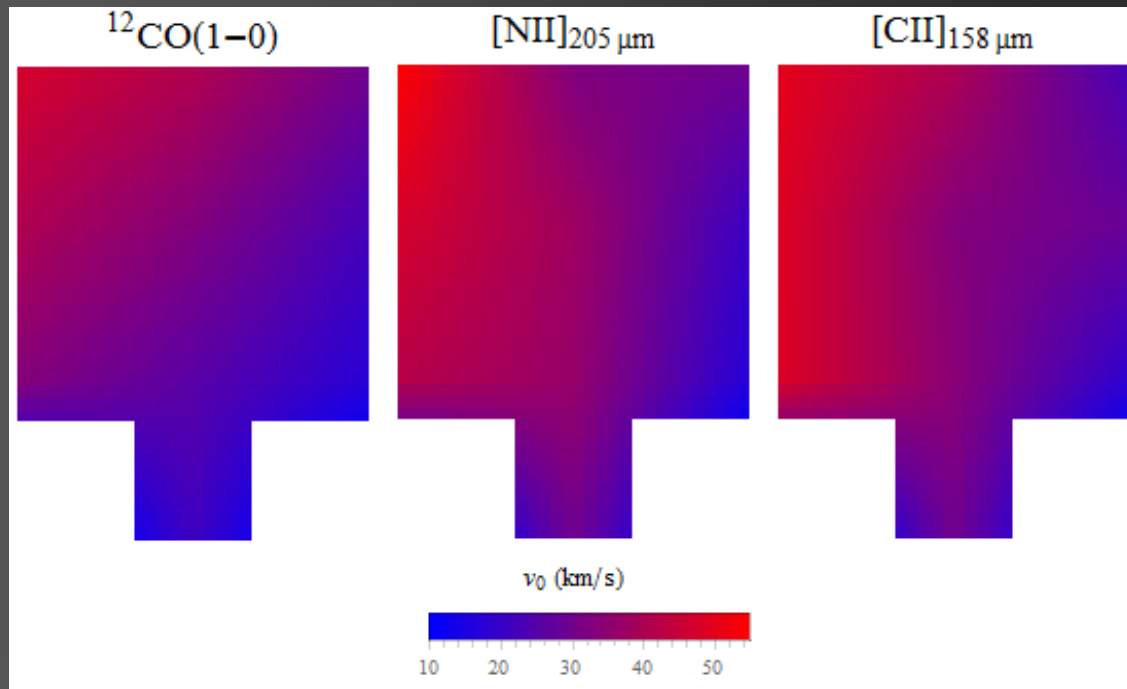
Kinematics: [CII], [NII] and $^{12}\text{CO}(1-0)$

line center velocities

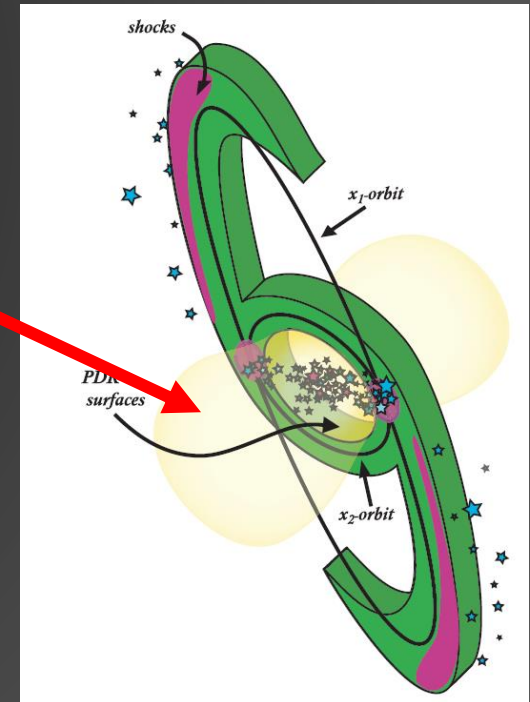


Kinematics: [CII], [NII] and $^{12}\text{CO}(1-0)$

line center velocities

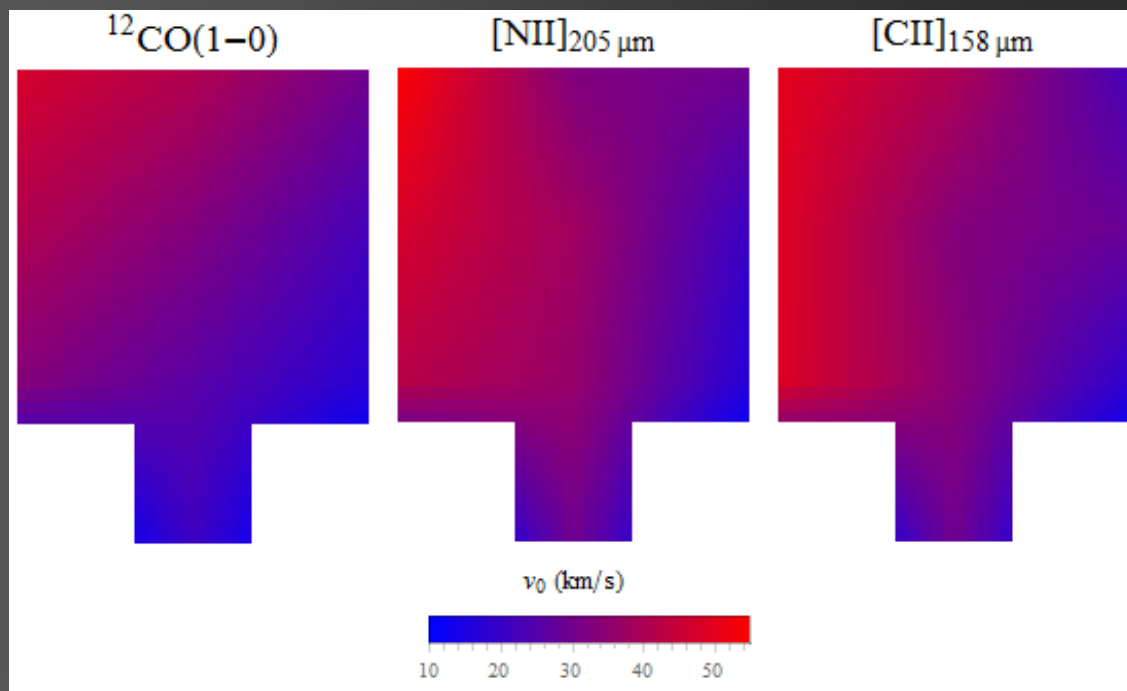


- Gaussian line center velocities are show spatial differences between CO, C^+ and N^+
- CO shows a clear velocity gradient from N-E to S-W
- BUT: This N^+ gas should be blue-shifted!

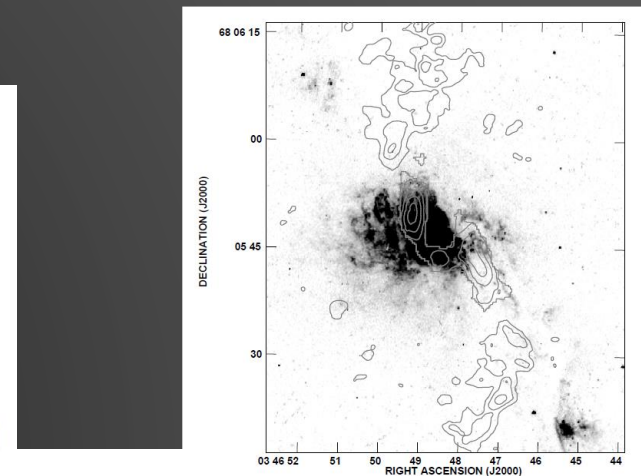
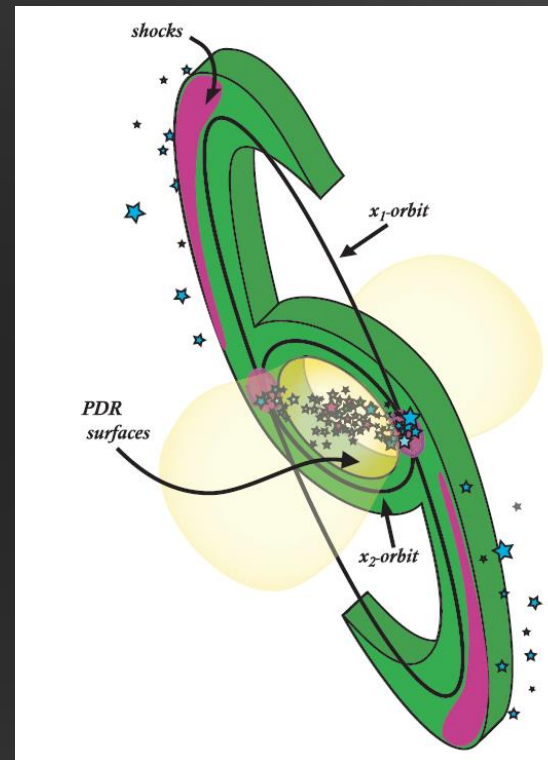


Kinematics: [CII], [NII] and $^{12}\text{CO}(1-0)$

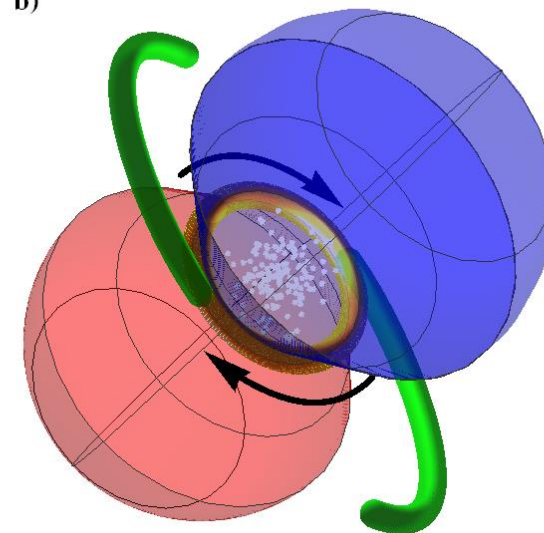
line center velocities



Doppler-shift of ionized gas challenges the geometrical model of the nucleus of IC 342.



b)

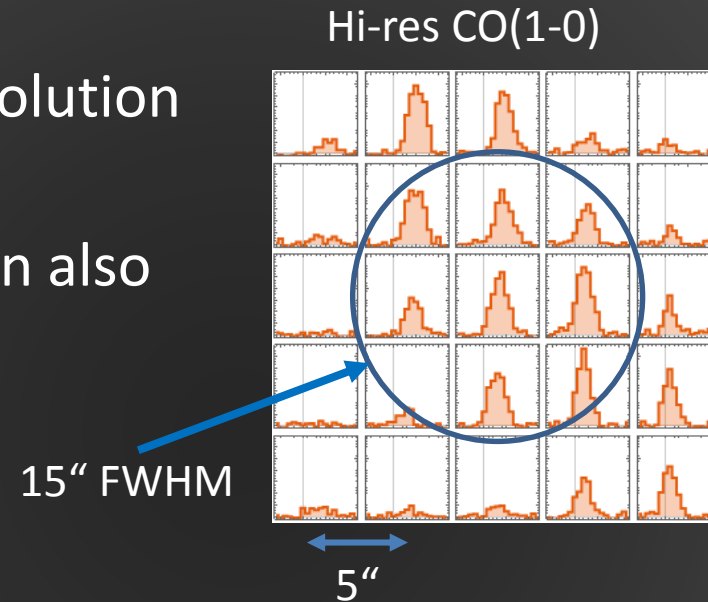


Super-resolution simulation

- The 15" SOFIA [CII] beam corresponds to $D > 240 \text{ pc}$
- The unresolved GMCs, PDRs, etc. in the beam pass their kinematic signature on to the observed, beam convolved [CII] spectrum.
- If we had access to kinematic information with higher angular resolution, we could analyze how the unresolved structures need to be distributed to result in the observed spectral line shape.
- There is no [CII] data with higher angular resolution.
- **But there is interferometric CO data available with resolution $\leq 5''$**

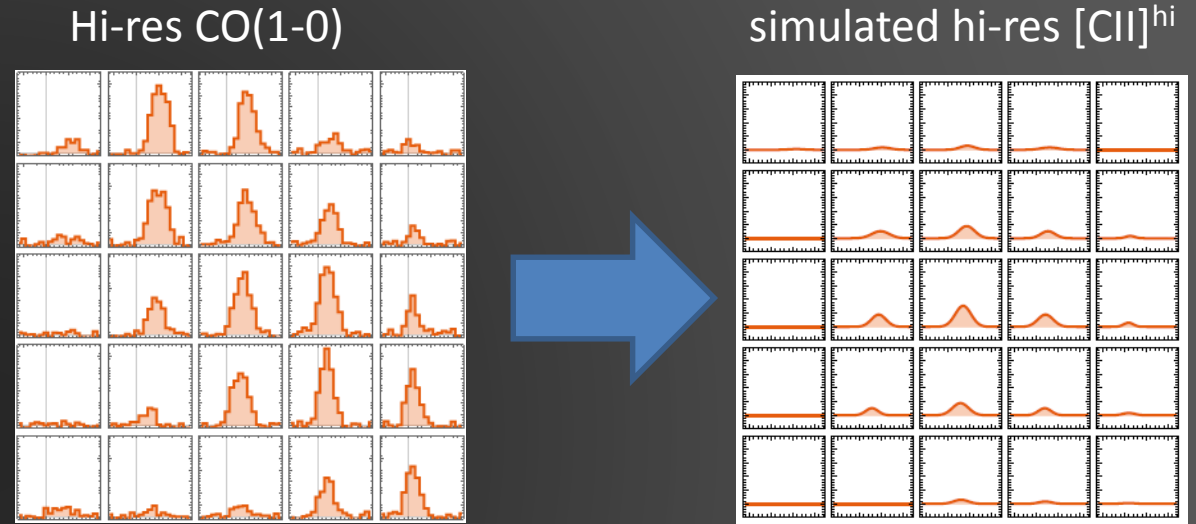
Sub-beam [CII]-CO correlation

- CO data with higher angular resolution than [CII] is available.
- We assume a [CII]-CO correlation also on very small scales.



Sub-beam [CII]-CO correlation

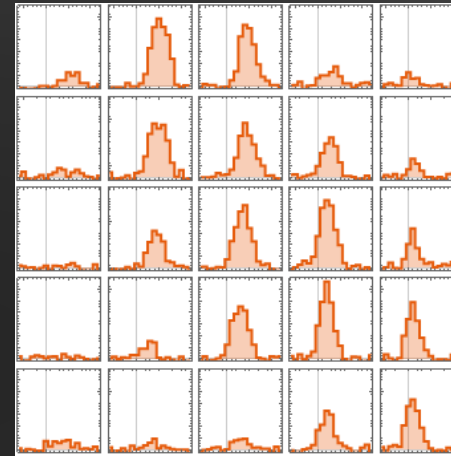
- CO data with higher angular resolution than [CII] is available.
- We assume a [CII]-CO correlation also on very small scales.
- We model artificial $[\text{CII}]^{\text{hi}}$ assuming FWHM_{CO} and $v_{0,\text{CO}}$



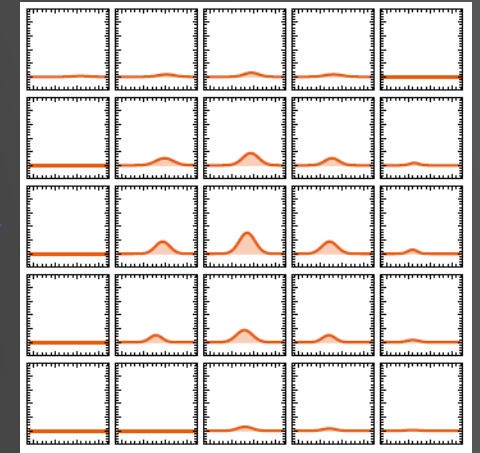
Sub-beam [CII]-CO correlation

- CO data with higher angular resolution than [CII] is available.
- We assume a [CII]-CO correlation also on very small scales.
- We model artificial $[\text{CII}]^{\text{hi}}$ assuming FWHM_{CO} and $v_{0,\text{CO}}$
- Simulate observation by convolving with 15" beam $[\text{CII}]^{\text{hi}} \Rightarrow [\text{CII}]^{\text{lo}}$

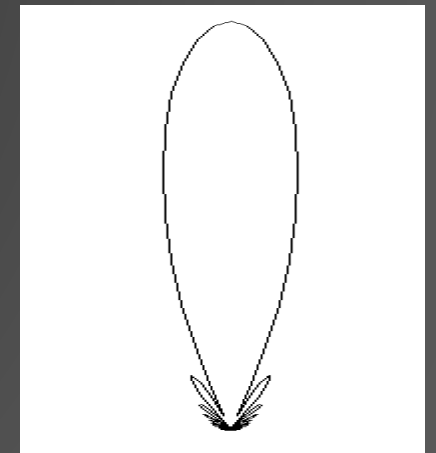
Hi-res CO(1-0)



simulated hi-res $[\text{CII}]^{\text{hi}}$



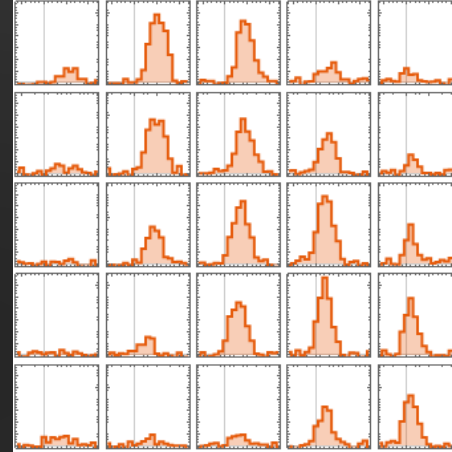
Convolve w. beam



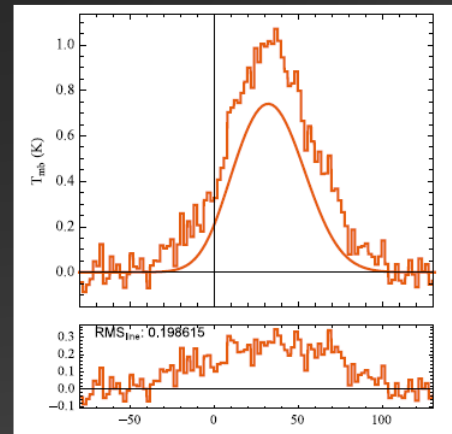
Sub-beam [CII]-CO correlation

- CO data with higher angular resolution than [CII] is available.
- We assume a [CII]-CO correlation also on very small scales.
- We model artificial $[\text{CII}]^{\text{hi}}$ assuming FWHM_{CO} and $v_{0,\text{CO}}$
- Simulate observation by convolving with 15" beam $[\text{CII}]^{\text{hi}} \Rightarrow [\text{CII}]^{\text{lo}}$
- Compare beam convolved $[\text{CII}]^{\text{low}}$ with $[\text{CII}]_{\text{obs}}$

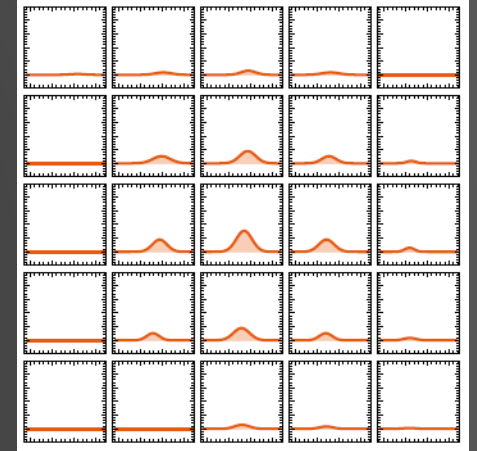
Hi-res CO(1-0)



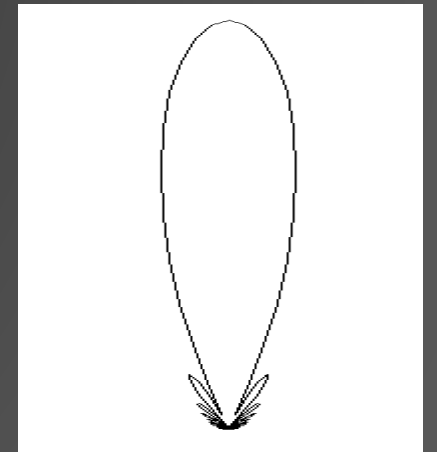
Simulated observation



simulated hi-res $[\text{CII}]^{\text{hi}}$

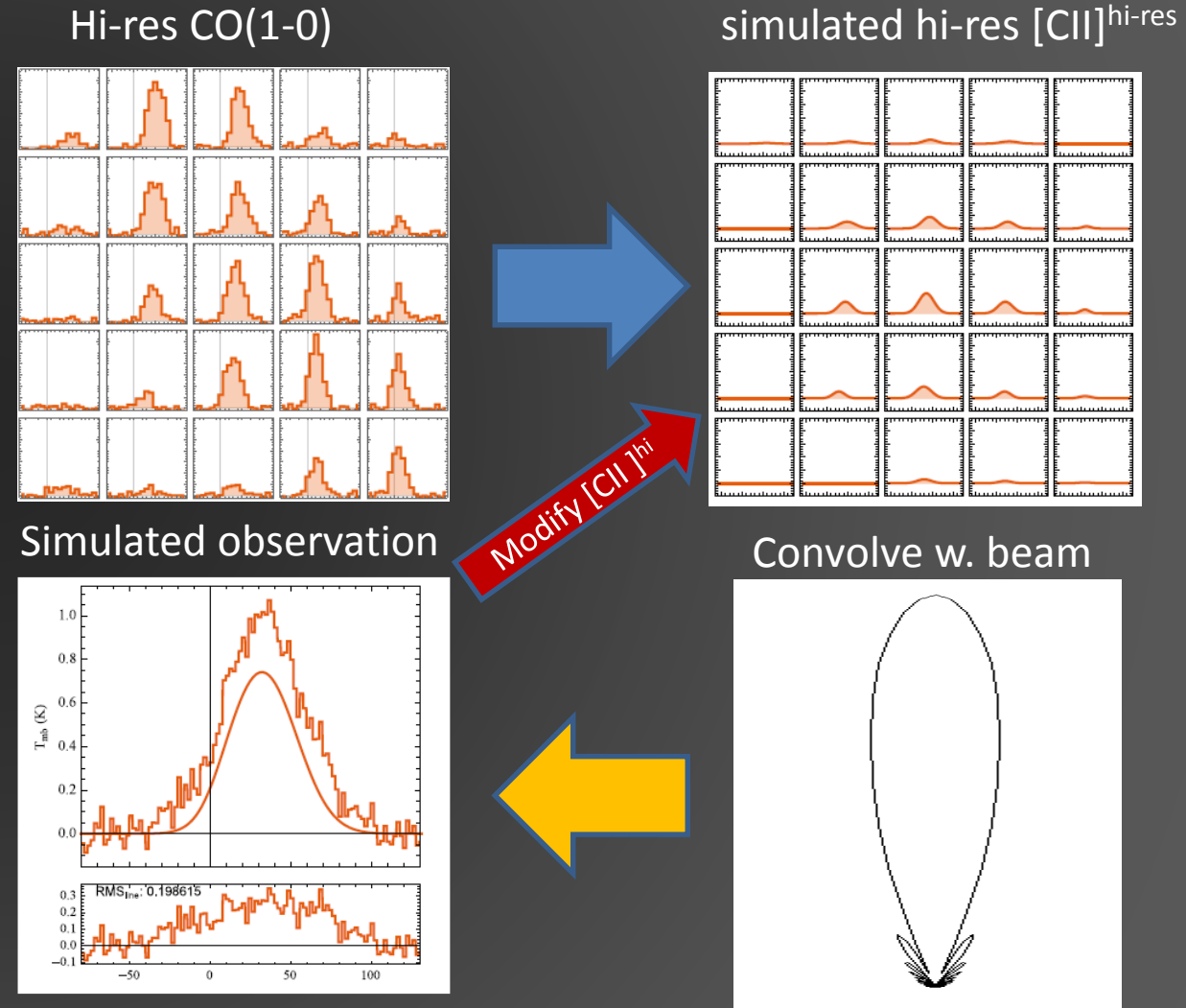


Convolve w. beam



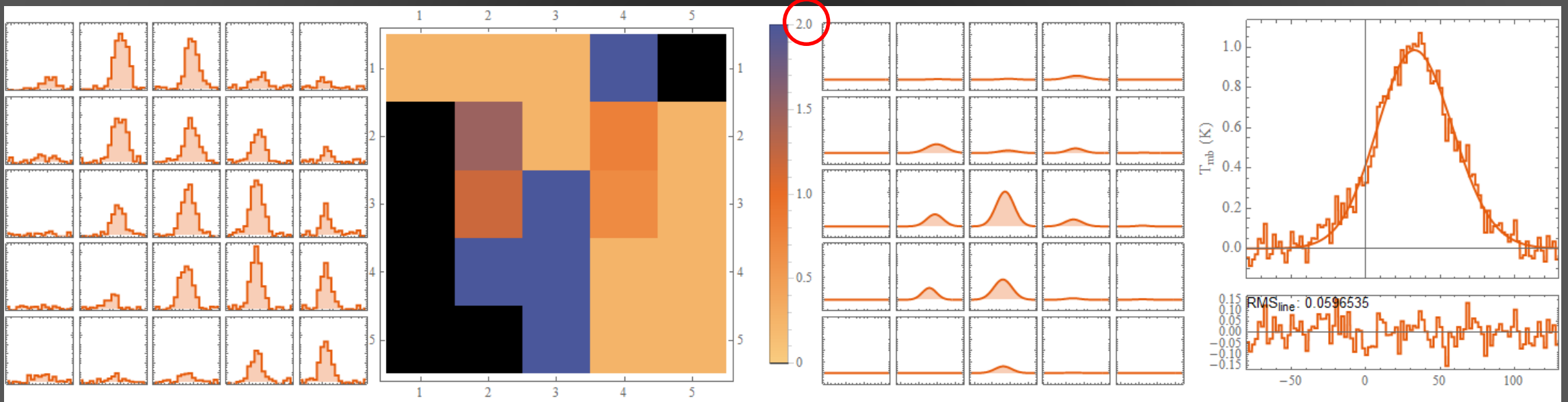
Sub-beam [CII]-CO correlation

- CO data with higher angular resolution than [CII] is available.
- We assume a [CII]-CO correlation also on very small scales.
- We model artificial $[\text{CII}]^{\text{hi-res}}$ assuming FWHM_{CO} and $v_{0,\text{CO}}$
- Simulate observation by convolving with beam $[\text{CII}]^{\text{hi-res}} \Rightarrow [\text{CII}]^{\text{lo-res}}$
- Compare beam convolved $[\text{CII}]^{\text{lo-res}}$ with $[\text{CII}]_{\text{obs}}$
- Modify $[\text{CII}]^{\text{hi-res}}$
- Rinse and repeat



[CII] Super-Resolution Composition

Constrained fit with max. T_{peak}



$T_{\text{peak}}([\text{CII}])$ @ each position

$[\text{CII}]^{\text{hi}}$ are already weighted
with Gaussian kernel

residuum

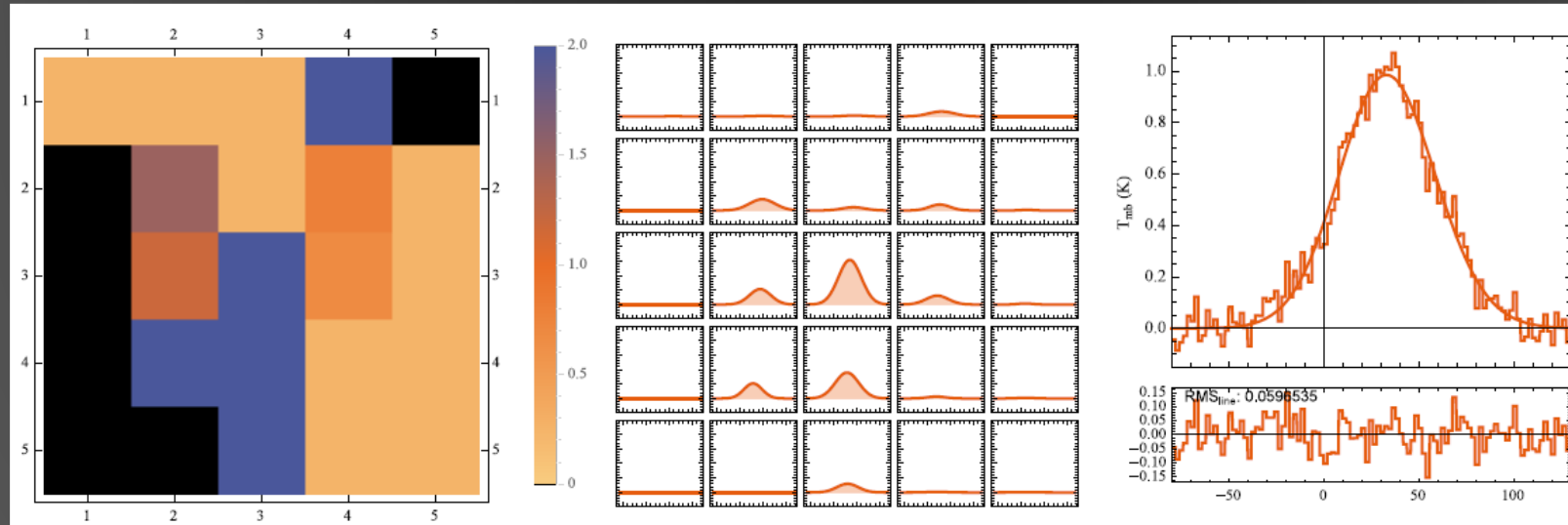
[CII] Super-Resolution Composition

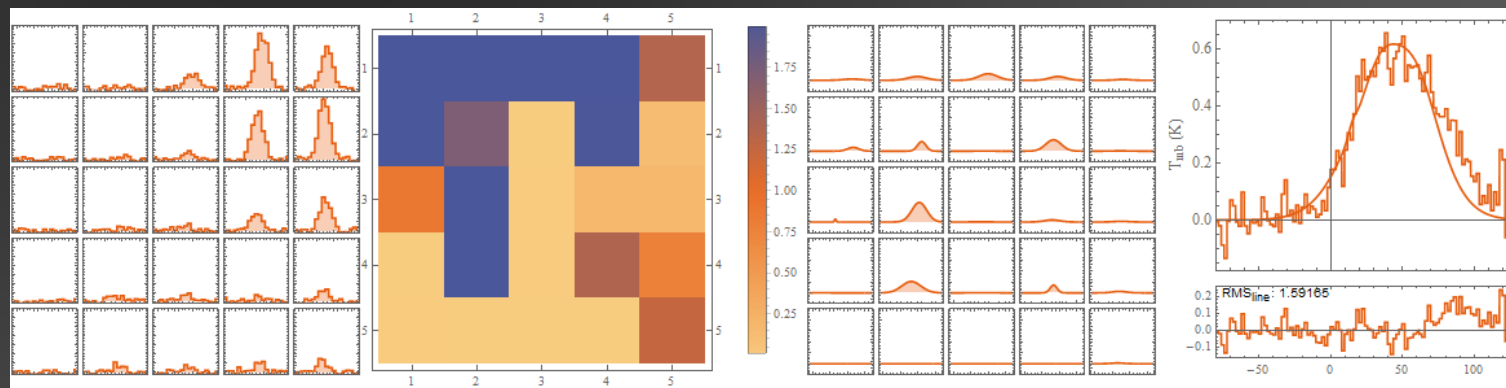
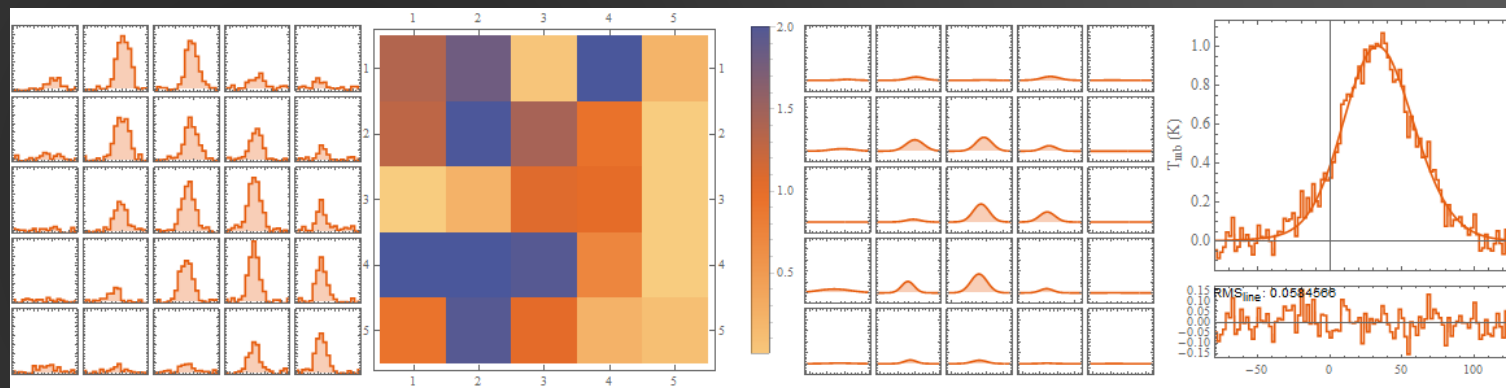
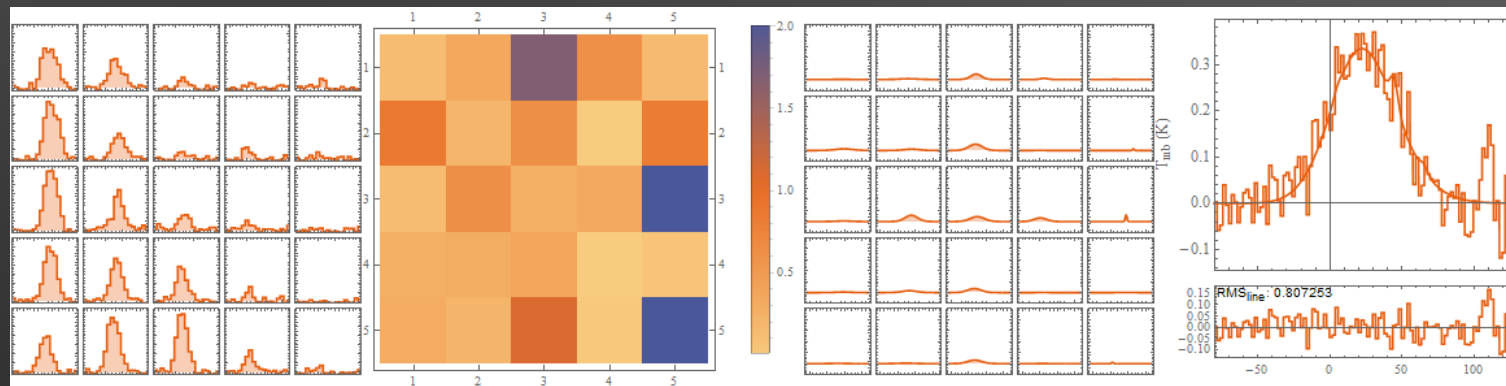
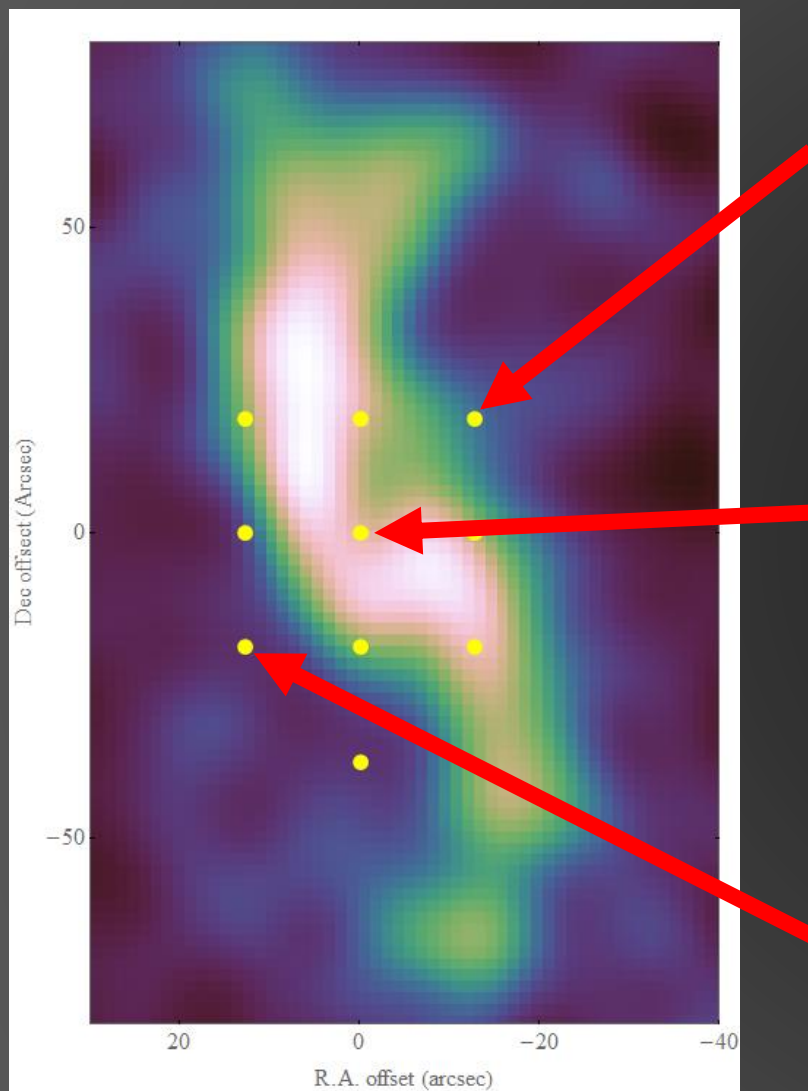
- Numerical fitting with 25(+1) degrees of freedom of varying weight is challenging
- The weaker the velocity gradient across the CO-map is, the higher the degeneracy between the parameters
→ kinematic influence of one CO position can be substituted by other positions with matching line shape.
- Qualitative conclusions difficult → the initial goal of a super-resolved map of numeric [CII]/CO ratios not yet reached.
- Quantitative conclusions already possible

→ We find the same qualitative trends in the super-resolved [CII]/CO distribution with complementary methods

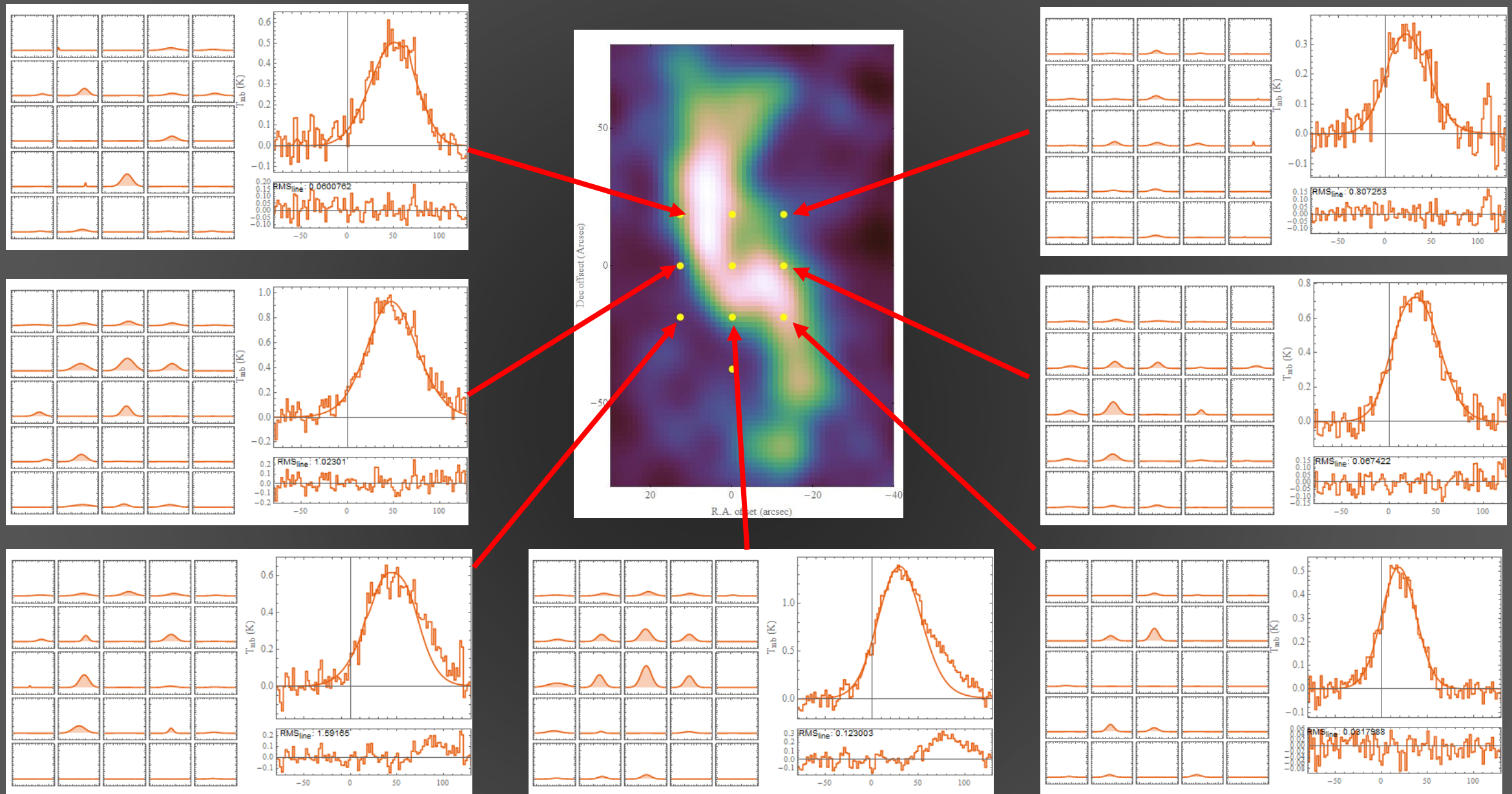
[CII] Super-Resolution Composition

- The kinematics of the observed [CII] emission is consistent with a scenario where the lower-left quadrant of the spiral/ring structure is dominantly contributing to the total [CII] emission. The gas along the northern arm is kinematically speaking of much less influence.





[CII] and [NII] emission in IC342 - The 6th Zermatt ISM Symposium - 7. Sep. 2015



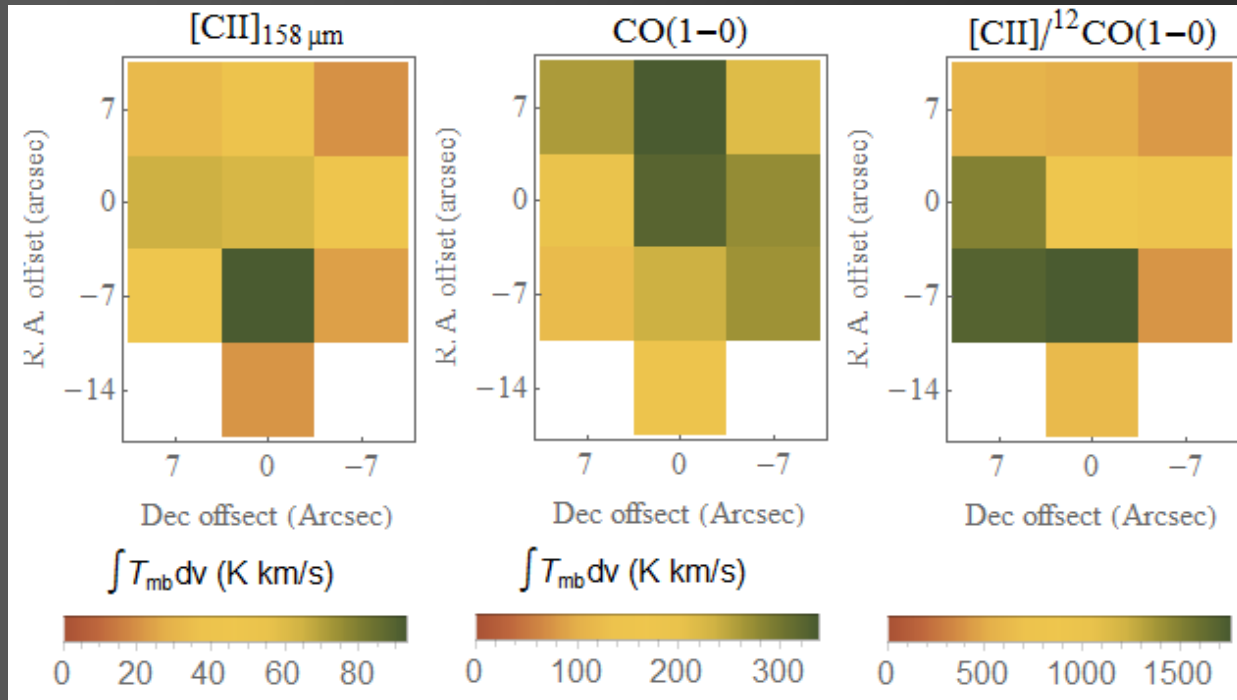
[CII] and [NII] emission in IC342 - The 6th Zermatt ISM Symposium - 7. Sep. 2015

Summary

- $[\text{CII}]_{158\mu\text{m}}$ and $[\text{NII}]_{205\mu\text{m}}$ detected in the nucleus of IC 342.
- The high angular and spectral resolution reveals a complex distribution of quiescent gas and PDR/starburst activity in the region.
- Strong starburst/PDR activity in the S-E consistent with complementary studies.
- The kinematic information of the emission from the ionized gas leads us to a refined geometrical concept of the center region of IC 342 (leading vs. trailing arms).
- Super-resolution method can be used to convolve the kinematic information from correlated data with very high-res. into a simulated observation in order to gain additional knowledge on the details of the assumed correlation.

Thank you!

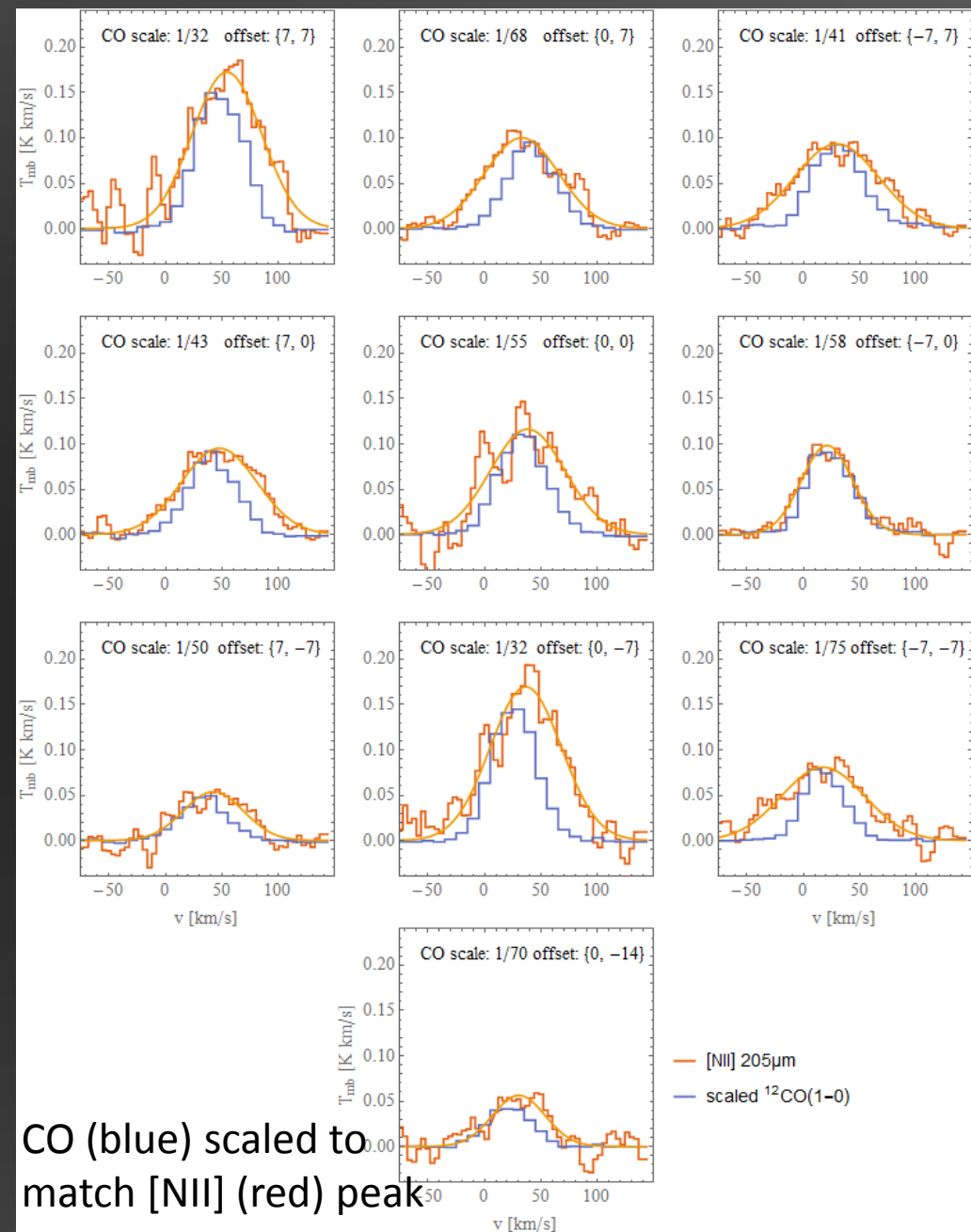
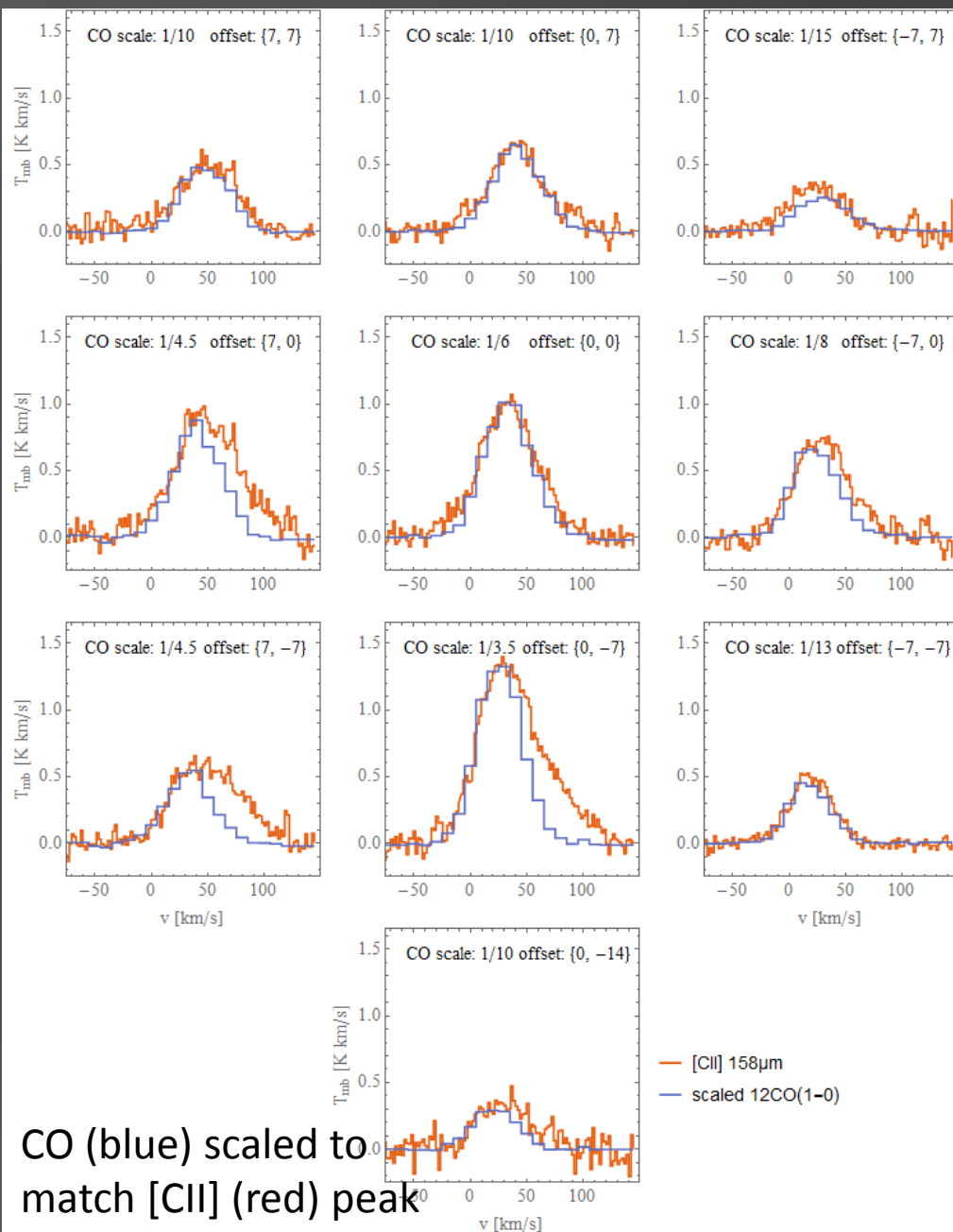
[CII] to CO ratio



Röllig et al. 2015

Direct comparison of line integrated intensities (single-component):

- [CII] emission strongest in the S-E quadrant
- [CII]/CO ratio highest in the S-E of our 3x3 grid.
- Local variations in the [CII]/CO ratio indicate spatial variations of the PDR/star formation activity along the molecular ring and mini-spiral.

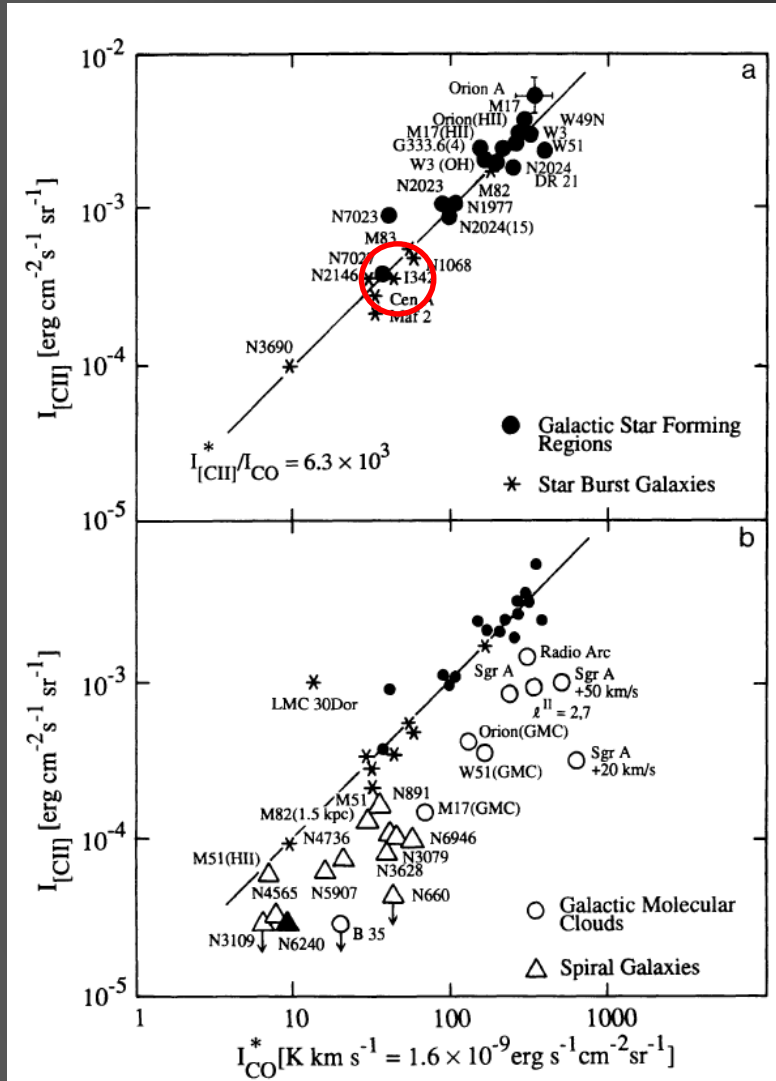


[CII]/CO as star formation tracer



- The intensity ratio $[\text{CII}]/^{12}\text{CO}(1-0)$ is often used as tracer of star formation/PDR/star burst activity
- $[\text{CII}]$ emission scales with FUV illumination
- Stronger FUV illumination from massive stars leads to stronger $[\text{CII}]$
- CO forms in the cool, shielded parts of the ISM
- Stronger FUV illumination leads to a decrease in $N(\text{CO})$ together with a reduced area filling factor

[CII]/CO as star formation tracer

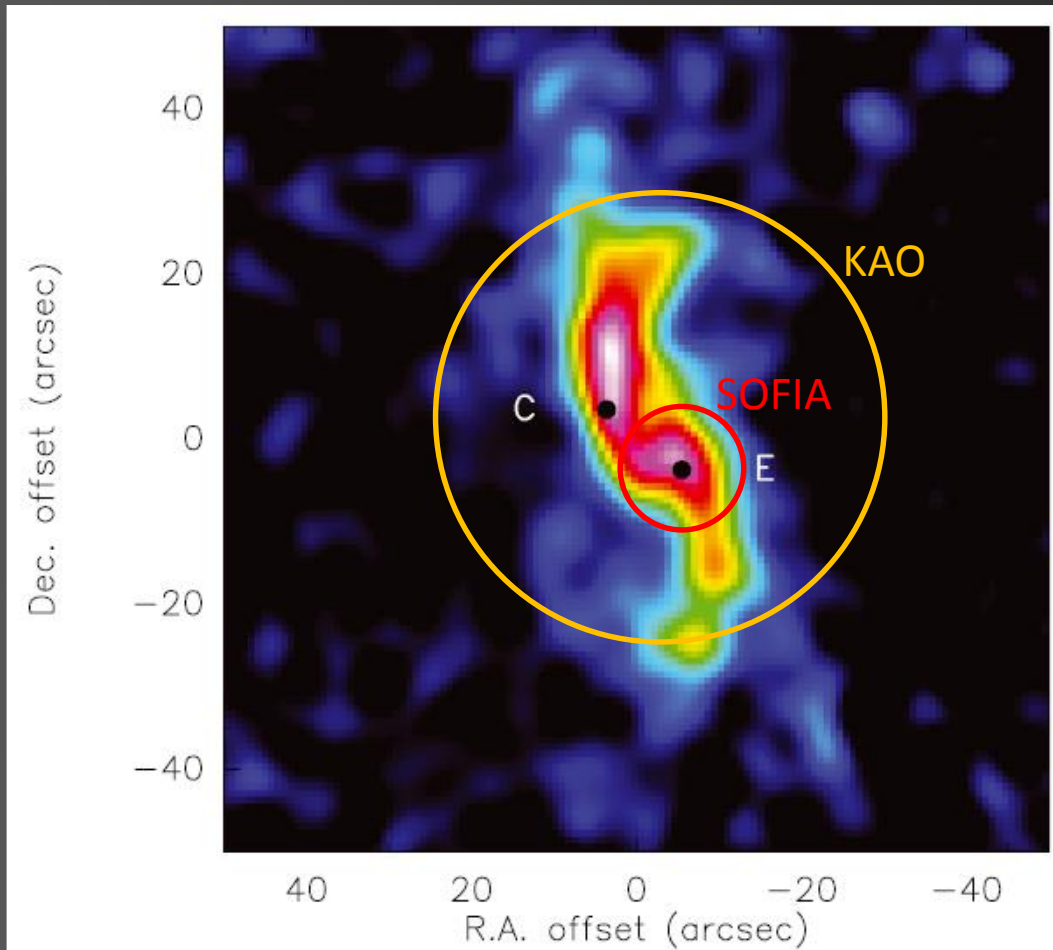


- $I_{[CII]}/I_{CO}=4000\text{-}6000$ is indicative of strong PDR activity/star bursts
- $I_{CO}=37.7\pm1.8$ K km/s @ 65" beam (NRAO, Rickard & Blitz 1985)
- $I_{[CII]}=3\times10^{-4}$ erg/s/cm²/sr @ 55" beam (KAO, Crawford et al. 1985)

Compare with higher resolution data

- $I_{CO}=302$ K km/s @ 15" (BIMA, smoothed)
- $I_{[CII]}=4.1\times10^{-4}$ erg/s/cm²/sr @ 15" (SOFIA)

KAO compared to SOFIA

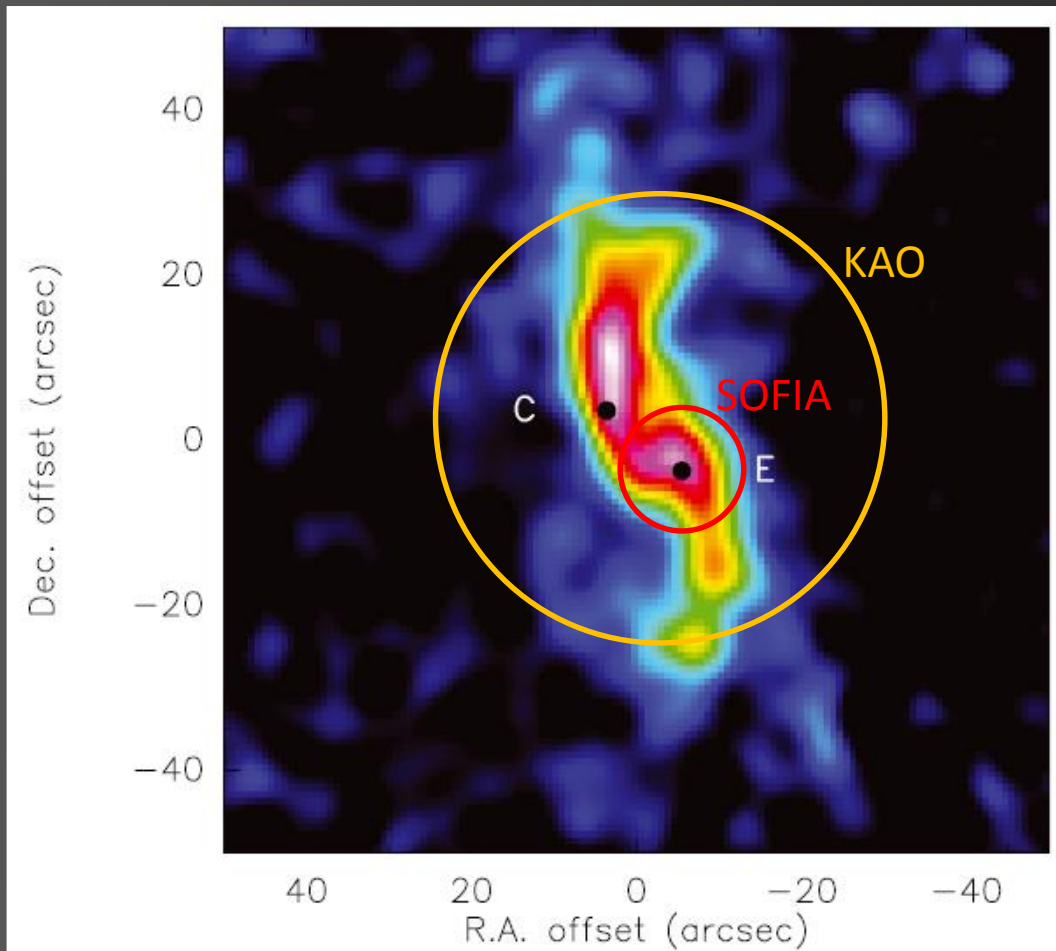


Stacey et al. 1991: $[\text{CII}]/\text{CO}=5000$

	GMC C	GMC E
$[\text{C II}]/^{12}\text{CO}(1-0)$	482	4236/692
$[\text{C II}]/^{12}\text{CO}(2-1)$	142	1223/150
$[\text{C I}]/^{12}\text{CO}(1-0)$	6.5	-/9.4
$[\text{C I}]/^{12}\text{CO}(2-1)$	1.9	-/2.4
$^{12}\text{CO}(4-3)/^{12}\text{CO}(1-0)$	20.7	21.1(-)
$N_{[\text{CII}]}/[10^{17}\text{cm}^{-2}]^a$	1.4	0.9/1.6
PDR model results		
$\langle n \rangle [10^3 \text{cm}^{-3}]$	5.0	10/2.0
$M_{\text{tot}} [10^6 M_{\odot}]$	20	2.0/15
$\chi [\text{Draine}]$	7	300/5

As always: higher angular resolution leads to a more complex picture.

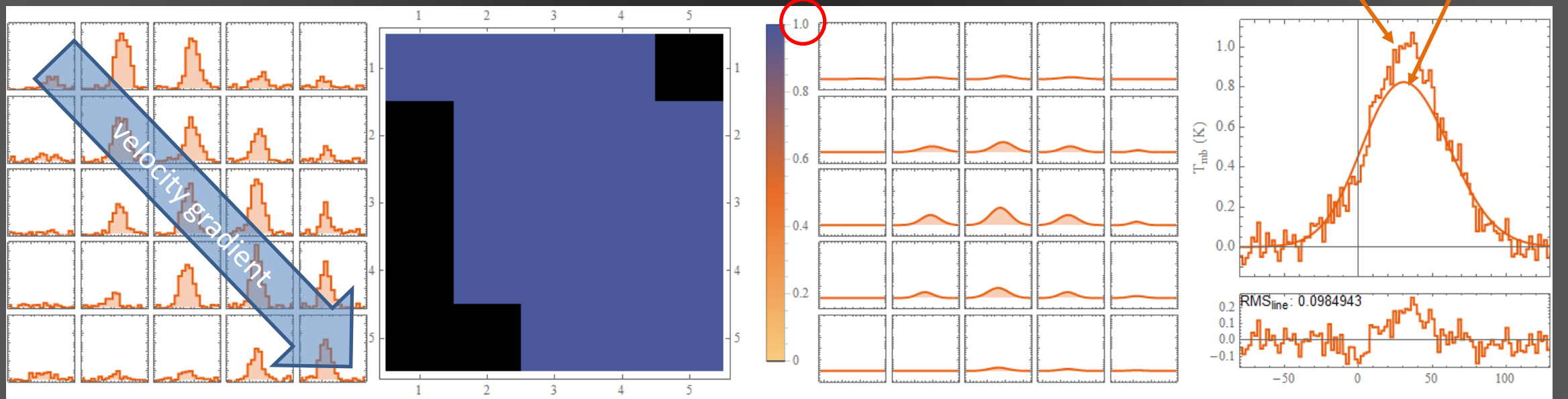
KAO compared to SOFIA



- [CII] and CO emission has a significantly different area filling factor
- C^+ has wider distribution.
- CO is concentrated toward the cool, shielded portion of the ISM
- Diffuse clouds with very little CO and much C^+ fill up the beam.
- With higher angular resolution we expect the [CII]/CO ratio to decrease.

[CII] Super-Resolution Composition

Constrained fit with max. T_{peak}



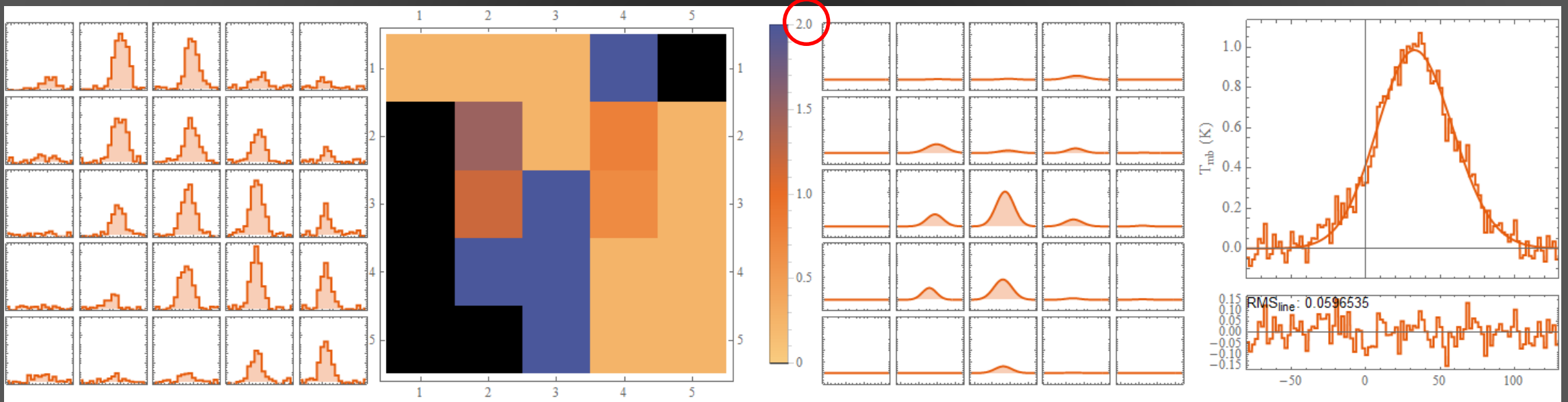
$T_{\text{peak}}([\text{CII}])$ @ each position

$[\text{CII}]^{\text{hi-res}}$ are already weighted
with Gaussian kernel

residuum

[CII] Super-Resolution Composition

Constrained fit with max. T_{peak}



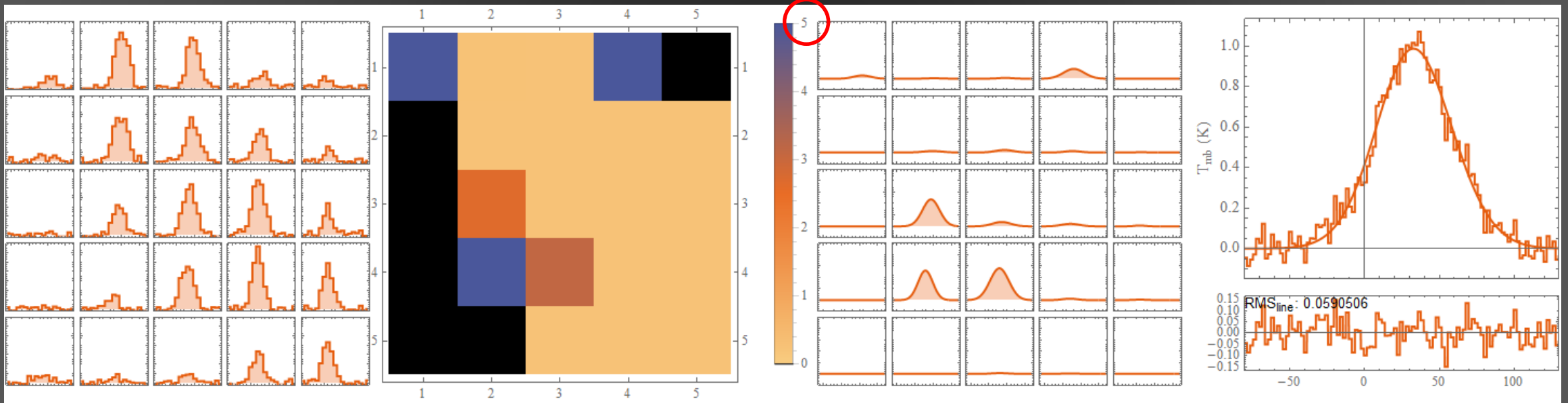
$T_{\text{peak}}([\text{CII}])$ @ each position

$[\text{CII}]^{\text{hi}}$ are already weighted
with Gaussian kernel

residuum

[CII] Super-Resolution Composition

Constrained fit with max. T_{peak}

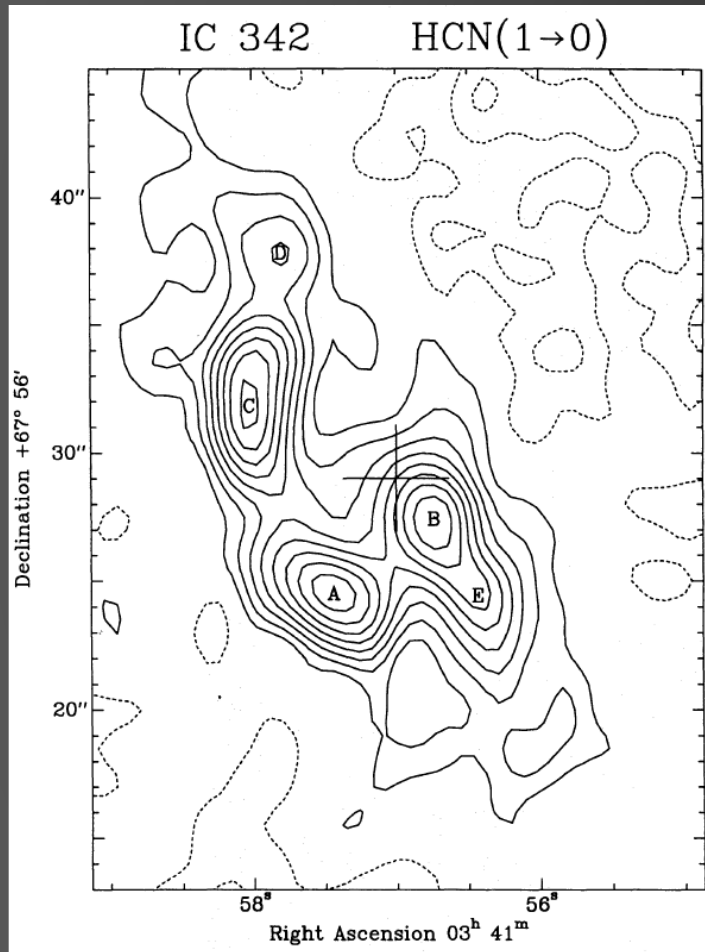


$T_{\text{peak}}([\text{CII}])$ @ each position

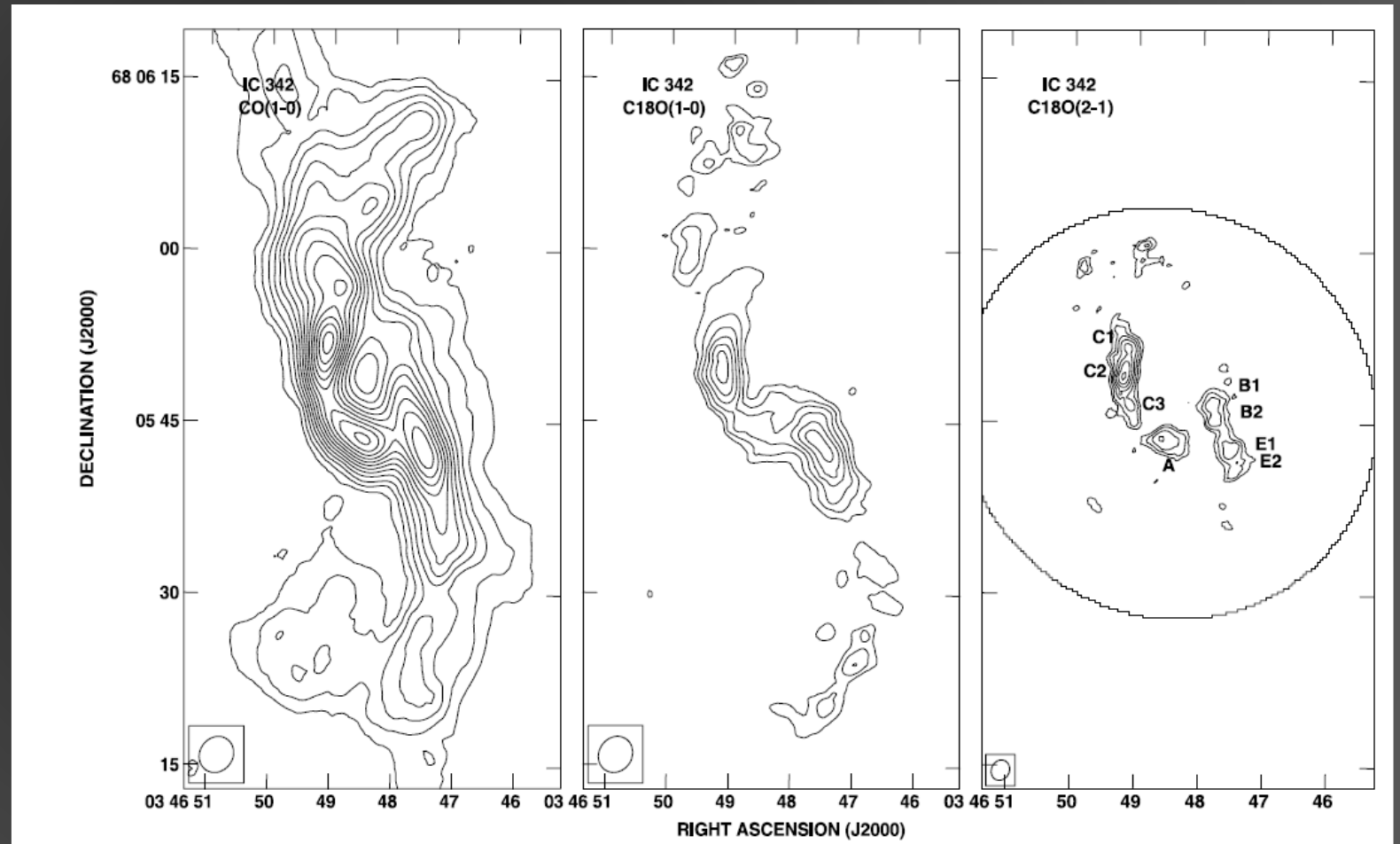
$[\text{CII}]^{\text{hi}}$ are already weighted
with Gaussian kernel

residuum

The Nucleus of IC 342



Downes et al. 1992



Meier & Turner 2001